Dynamics of $4D$ symplectic maps near a double resonance

V. Gelfreich[1], C. Simó[2] and A. Vieiro[2]

[1] Mathematics Institute, University of Warwick, Coventry CV4 7AL, UK

v.gelfreich@warwick.ac.uk

[2] Departament de Matemàtica Aplicada i Anàlisi,

Universitat de Barcelona, Gran Via 585, 08007 Barcelona, Spain

carles@maia.ub.es vieiro@maia.ub.es

May 17, 2012

Abstract

We study the dynamics of a family of $4D$ symplectic mappings near a doubly resonant elliptic fixed point. We derive and discuss algebraic properties of the resonances required for the analysis of a Takens type normal form. In particular, we propose a classification of the double resonances adapted to this problem, including cases of both strong and weak resonances.

Around a weak double resonance (a junction of two resonances of two different orders, both being larger than 4) the dynamics can be described in terms of a simple (in general non-integrable) Hamiltonian model. The non-integrability of the normal form is a consequence of the splitting of the invariant manifolds associated with a normally hyperbolic invariant cylinder.

We use a $4D$ generalisation of the standard map in order to illustrate the difference between a truncated normal form and a full $4D$ symplectic map. We evaluate numerically the volume of a $4D$ parallelotope defined by 4 vectors tangent to the stable and unstable manifolds respectively. In good agreement with the general theory this volume is exponentially small with respect to a small parameter and we derive an empirical asymptotic formula which suggests amazing similarity to its $2D$ analog.

Different numerical studies point out that double resonances play a key role to understand Arnold diffusion. This paper has to be seen, also, as a first step in this direction.

Contents

1 Introduction

It is generally accepted that resonant phenomena play an important role in the theory of Hamiltonian systems and its applications. An important example is the Nekhoroshev theory which provides an upper bound on the rate of Arnold diffusion. In this theory the analysis of dynamics near resonances of higher orders is at the centre of the argument [1, 2]. Several numerical studies [5, 6, 7, 8] support the fact that multiple resonances should play an important role in an explanation of the Arnold diffusion [3]. While along a simple resonance, crossed by high or very high order resonances, the main tool is the well-known transition chain mechanism [9]. Then, the main effect of the resonance is to create a "pendulum-like" system and, hence, integrable. In the case of multiple resonances they create locally, even in the simplest approximation, a Hamiltonian system with two or more degrees of freedom, generically non-integrable.

Resonances usually appear in one of the following contexts:

- small perturbations of an integrable system,
- small oscillations near an equilibrium,
- small oscillations near a periodic orbit.

In the last case the dynamics can also be described by a Poincaré map near its fixed point. In each one of these cases, the normal form theory provides a powerful tool for the study of the local dynamics [4].

Each resonance can be characterised by a number of independent resonant relations between the frequencies, this number being called the *multiplicity of the resonance*. In the case of a simple resonance the normal form is integrable, while a double resonance can lead to non-integrability (see e.g. the book [10]). In particular, in a near-integrable system with three or more degrees of freedom the dynamics near a double resonance can be described by a two degrees of freedom Hamiltonian system, which has the form of a sum of a quadratic form in action variables plus a periodic potential [4]. In general this normal form does not contain any perturbation parameter, a fact that substantially complicates its analysis. Haller [10] showed non-integrability of the corresponding normal form in the case when one of the two fundamental resonances has a relatively small amplitude compared to the other one. This situation should generically arise if one of the resonances has a very high order [11, 10]. On the other hand this assumption is not expected to be satisfied if both fundamental resonances are of comparable orders.

In this paper we provide a detailed analysis of the normal form near a fixed point of a $4D$ symplectic map. It extends and completes the original analysis carried out in [12]. We provide a more detailed classification of the cases with different dynamical behaviour in the normal form.

The paper is structured in the following way. In the next section we provide mostly known results on the classification of the resonances, describe the Takens normal form adapted to the Hamiltonian set up, and analyse the symmetries of the normal form Hamiltonian. In Section 3 we discuss arithmetic properties of the double resonances which can be considered as a two dimensional sub-lattice of $\mathbb{Z}^2$. In particular, we prove that all the resonances can be generated by two independent resonances of the lowest orders, which we call *minimal generators*. These pairs are not unique. For a majority of resonances this non-uniqueness is rather trivial – it originates from the symmetry of the set of resonances with respect to the reflection around the origin. But for some frequencies the non-uniqueness is not trivial and it is reflected in a more complicated structure of a normal form truncated at the order corresponding to the lowest resonant order.

We will also show that for some frequencies two independent resonances of the lowest possible orders may or may not generate all other resonances, and we shall establish sufficient conditions to ensure they do it. The cases when the minimal generators are not unique are discussed in Section 3.4.

In Section 3.2 we provide the complete list of eigenvalues which lead to two independent resonance relations of order 3 or 4. We call them *doubly strong resonances*, since their normal form has no integrable approximation.

In Section 4 we show that a weak double resonance has (in general) a non-integrable normal form. Earlier Kovacic [13] and Haller [14] performed a similar analysis for a nearly integrable system. That analysis required a set of additional hypothesis on the amplitudes of the coefficients in the normal form, which cannot be guaranteed for a generic system. In particular, to ensure such a decay of the coefficients, they obtain a model to describe the dynamics at the junction of the two resonances that requires them to be of quite different order. In this paper, using a similar method, we arrive to more generic conclusions because we take advantage of the properties of the normal form near a fixed point. As a consequence, the (non-integrable) model we obtain from the normal form describes the dynamics in a suitable vicinity around the junction of the resonances provided they are of different order, including the case of similar orders.

Our numerical experiments also have some unusual consequences. Indeed, numerically it can be difficult to distinguish between a very smooth and an analytical invariant surface. On the other hand, it is well known that the general theory of normal hyperbolicity guaranties the existence of invariant manifolds which are smooth, but it is expected that they are not analytic. We provide a strong numerical evidence that a normally hyperbolic invariant cylinder of the truncated normal form is not analytic and has the degree of regularity expected from empirical arguments. The details are placed in Section 4.2. We note that similar experiments can be conducted with a $4D$ standard-like map used in this paper as a model for the dynamics near a double resonance.

In Section 5 we analyse numerically the difference between an original map and its normal form. We take the $4D$ standard-like map introduced before as a model and we study the splitting of the invariant manifolds of its hyperbolic fixed point. We find several primary homoclinic points. Our numerical study shows that these points are transversal. Moreover, we show that a suitable volume taken as a measure of transversality becomes exponentially small in the bifurcation parameter. Such an exponentially small behaviour follows indeed from the standard suspension and averaging techniques since the map is near-the-identity [28, 29], see related comments in Section 5. Note that as the normal form is given by a Hamiltonian flow, the preservation of the energy of the Hamiltonian implies that such a volume is zero in the normal form case. Furthermore, we found an empirical formula for the asymptotic behaviour of such splitting which resembles the well studied $2D$ case. This suggests that the methods developed for the study of two dimensional maps can be extended to higher dimensions, although we are not aware of any analytical result in this direction.

2 Resonant Normal Forms

2.1 Classification of resonances

In this paper we carry out the analysis of the normal forms for a 4-dimensional symplectic map near a totally elliptic fixed point. More precisely, we consider a two-parametric family of $4D$ symplectic maps $F_{\boldsymbol{\delta}}$ which depend on a small enough vector parameter $\boldsymbol{\delta} = (\delta_1, \delta_2)$. We assume that the maps have a fixed point at the origin for all $\boldsymbol{\delta}$

$$F_{\boldsymbol{\delta}}(\mathbf{0}) = \mathbf{0}$$

and $DF_{\mathbf{0}}(\mathbf{0})$ has four non-real eigenvalues on the unit circle $\lambda_1, \bar{\lambda}_1, \lambda_2, \bar{\lambda}_2$. Without losing in generality, we may assume that $\operatorname{Im} \lambda_k > 0$. Then there exist $\alpha_k \in (0, \frac{1}{2})$ such that $\lambda_k = \exp(2\pi i \alpha_k)$, $k = 1, 2$. In this paper we will always assume that the eigenvalues are simple, i.e., $\alpha_1 \neq \alpha_2$.

The local dynamics of the map can be described in terms of a normal form which depends on the arithmetic properties of α_k in an essential way. More precisely, the normal form is determined by the set of resonances which form a subgroup $\Gamma \subset \mathbb{Z}^2$ defined by

$$\Gamma = \{\, (k_1, k_2) : k_1\alpha_1 + k_2\alpha_2 = 0 \pmod 1 \,\}\,. \tag{2.1}$$

We say that $\mathbf{r} = (k_1, k_2) \in \Gamma$ is *a resonance of order* $|\mathbf{r}| = |k_1| + |k_2|$. We note that $(k_1, k_2) \in \Gamma$ if and only if

$$\lambda_1^{k_1}\lambda_2^{k_2} = 1\,. \tag{2.2}$$

Of course $(0, 0)$ is always resonant, and we call it the *trivial (or unavoidable) resonance.*

The fixed point of $F_{\mathbf{0}}$, at the origin, is of one of the following three types:

1. Non-resonant (Γ is a trivial group).
   In this case $\{\, \alpha_1, \alpha_2, 1 \,\}$ are rationally independent.

2. Simply resonant (Γ is a one-dimensional lattice).
   In this case there are two possibilities:
   a) $\alpha_1 \in \mathbb{Q}$, $\alpha_2 \in \mathbb{R} \setminus \mathbb{Q}$ (or vice versa).
   b) $\alpha_1, \alpha_2 \in \mathbb{R} \setminus \mathbb{Q}$ but $\{\, \alpha_1, \alpha_2, 1 \,\}$ are rationally dependent.

3. Doubly resonant (Γ is a two-dimensional lattice).
   In this case $\alpha_1, \alpha_2 \in \mathbb{Q}$ and we can write them in the form of irreducible fractions

$$\alpha_1 = \frac{p_1}{q_1} \qquad \text{and} \qquad \alpha_2 = \frac{p_2}{q_2}\,, \qquad p_1, p_2, q_1, q_2 \in \mathbb{N}\,.$$

It is well known that non-resonant and simply resonant normal forms are integrable due to the existence of a continuous family of symmetries. In the case of a double resonance the normal form is expected to be non-integrable and one of our goals is to understand what kind of dynamics can be expected there.

Obviously, both simply resonant and doubly resonant eigenvalues are dense in the torus

$$\mathcal{T} = \{\, (\lambda_1, \lambda_2) \in \mathbb{C}^2 : |\lambda_1| = |\lambda_2| = 1 \,\}.$$

We note that each resonant relation $\alpha_1 k_1 + \alpha_2 k_2 = k_3$, where $k_1, k_2, k_3 \in \mathbb{Z}$, defines a line on this torus. The Fig. 1 shows all the resonant lines up to the order 12. The picture represents one quarter of the torus. The whole torus can be obtained by reflecting with respect to the coordinate axes.

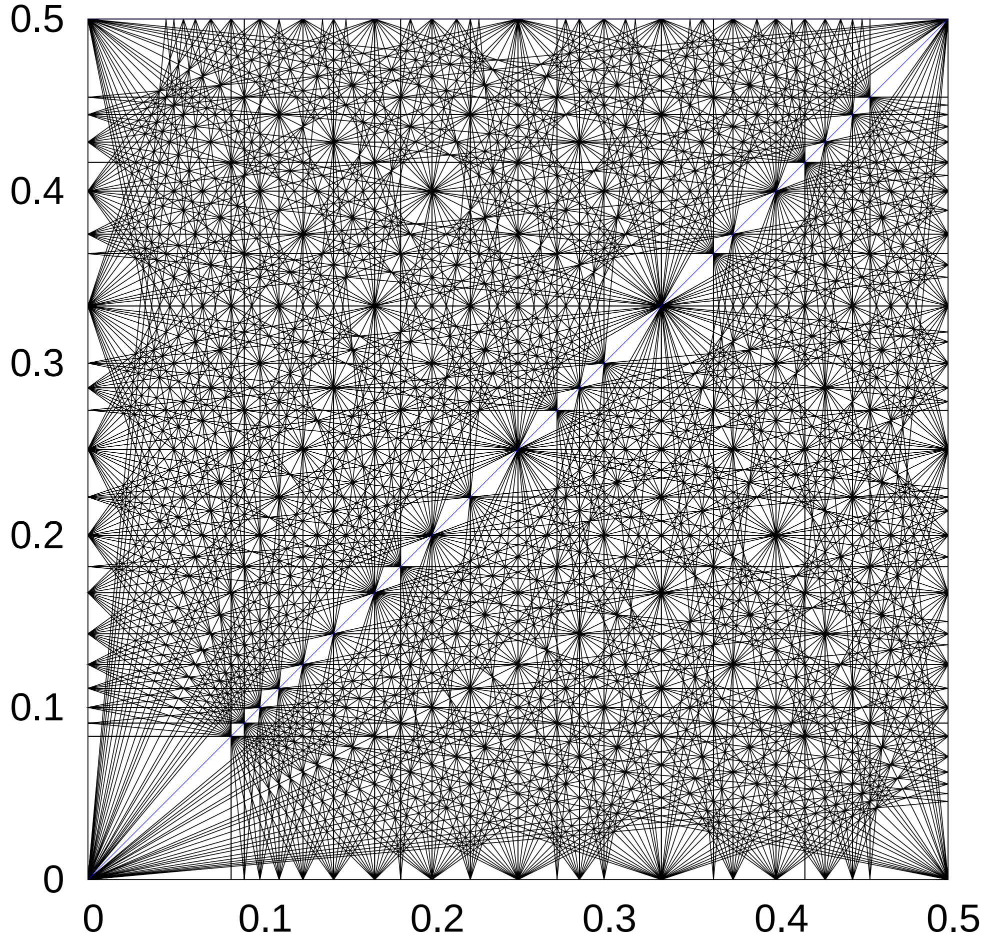

Figure 1: Resonant lines (of order ≤ 12) on the plane (α_1, α_2).

2.2 Takens Normal Form

Since the eigenvalues of the Jacobian matrix $DF_{\mathbf{0}}(\mathbf{0})$ are simple, it can be transformed into a linear map $\Lambda_{\mathbf{0}}$ which acts on a vector (x_1, y_1, x_2, y_2) by rotating (x_k, y_k) by the angle α_k respectively for $k = 1, 2$. Using a formal symplectic substitution we can transform $F_{\boldsymbol{\delta}}$ (as well as $F_{\mathbf{0}}$) into the Birkhoff normal form $N_{\boldsymbol{\delta}}$, which commutes with the linear map $\Lambda_{\mathbf{0}}$:

$$N_{\boldsymbol{\delta}} \circ \Lambda_{\mathbf{0}} = \Lambda_{\mathbf{0}} N_{\boldsymbol{\delta}}.$$

Since $N'_{\mathbf{0}}(\mathbf{0}) = \Lambda_{\mathbf{0}}$, the map $\Lambda_{\mathbf{0}}^{-1} N_{\boldsymbol{\delta}}$ is tangent to the identity and therefore there is a formal Hamiltonian $H_{\boldsymbol{\delta}}$ such that $\Lambda_{\mathbf{0}}^{-1} N_{\boldsymbol{\delta}} = \Phi^1_{H_{\boldsymbol{\delta}}}$ or equivalently

$$N_{\boldsymbol{\delta}} = \Lambda_{\mathbf{0}} \Phi^1_{H_{\boldsymbol{\delta}}}$$

where $\Phi^1_{H_{\boldsymbol{\delta}}}$ is a time-one map of $H_{\boldsymbol{\delta}}$. This Takens normal form [15, 16] is more convenient as it facilitates the analysis of the dynamics by providing an explicit expression for an integral of motion ($H_{\boldsymbol{\delta}}$). Of course, it is generally believed that the normal forms are formal, i.e., the series do not generically converge. In this sense, we remark that, in a suitable compact around the origin, using suspension and averaging techniques [28, 29], one can show that the difference between the optimally truncated normal form and the original map is bounded by a quantity which is exponentially small in the size of the domain. In particular, it follows that a suitable iterate of $F_{\boldsymbol{\delta}}$ can be approximately represented as a time-one map of a Hamiltonian flow with the approximation error being exponentially small. Moreover, this Hamiltonian has symmetries inherited from the symmetries of the normal form.

The normal form Hamiltonian $H_{\boldsymbol{\delta}}$ is $\Lambda_{\mathbf{0}}$-invariant:

$$H_{\boldsymbol{\delta}} = H_{\boldsymbol{\delta}} \circ \Lambda_{\mathbf{0}}.$$

This property is important as it implies $N^j_{\boldsymbol{\delta}} = \Lambda^j_{\mathbf{0}} \Phi^j_{H_{\boldsymbol{\delta}}}$ for all $j \in \mathbb{N}$ which allows to study the flow of $H_{\boldsymbol{\delta}}$ instead of iterations of $N_{\boldsymbol{\delta}}$.

It is useful to rewrite the normal forms in complex variables defined by

$$z_k = x_k + iy_k \quad \text{and} \quad \bar{z}_k = x_k - iy_k.$$

Note that (x_k, y_k) are pairs of canonically conjugated variables for $k = 1, 2$. In the $z_1, z_2, \bar{z}_1, \bar{z}_2$ coordinates $\Lambda_{\mathbf{0}}$ is given by:

$$DF_{\mathbf{0}}(\mathbf{0}) = \Lambda_{\mathbf{0}} = \operatorname{diag}(\lambda_1, \lambda_2, \bar{\lambda}_1, \bar{\lambda}_2)\,.$$

In the Hamiltonian normal form theory a monomial $z_1^j \bar{z}_1^k z_2^l \bar{z}_2^m$ is called *resonant* if it is $\Lambda_{\mathbf{0}}$-invariant or, equivalently, if $(j-k, l-m) \in \Gamma$ defined in (2.1). The normal form Hamiltonian is a formal sum of resonant monomials:

$$H_{\boldsymbol{\delta}} = \sum_{\substack{(j-k,l-m)\in\Gamma \\ j,k,l,m\geq 0}} h_{jklm}(\boldsymbol{\delta}) z_1^j \bar{z}_1^k z_2^l \bar{z}_2^m\,. \tag{2.3}$$

The Hamiltonian $H_{\boldsymbol{\delta}}$ represents a Hamiltonian system with two degrees of freedom which may be non-integrable. One of the goals of this paper is to show that this is generically true in the case of a double resonance.

In order to study the dynamics it is convenient to introduce symplectic polar coordinates by

$$I_j = \frac{|z_j|^2}{2}, \qquad \varphi_j = \arg z_j\,.$$

Substituting $z_j=(2I_j)^{1/2}e^{i\varphi_j}$ into the Hamiltonian (2.3) and combining pairs of complex conjugate terms we rewrite the Hamiltonian in the form

$$H_{\boldsymbol{\delta}}=\sum_{\substack{(k_1,k_2)\in\Gamma^+\\ p,q\geq 0}} a_{k_1k_2pq}(\boldsymbol{\delta})I_1^{p+k_1/2}I_2^{q+|k_2|/2}\cos(k_1\varphi_1+k_2\varphi_2+b_{k_1k_2pq})\,, \tag{2.4}$$

where Γ^+ is the subset of Γ which consists of all vectors of the form (k_1,k_2) with $k_1>0$ and all vectors $(0,k_2)$ with $k_2\geq 0$. The $b_{k_1k_2pq}$ are suitable phases and we can assume $b_{00pq}=0$ for all p,q without loosing in generality. We note that $a_{klpq}(\boldsymbol{\delta})$ are formal series in $\boldsymbol{\delta}$ and

$$a_{0001}(\mathbf{0})=a_{0010}(\mathbf{0})=0,$$

which reflects the fact that the linear part of the map $N_{\boldsymbol{\delta}}$ (and $F_{\boldsymbol{\delta}}$) is exactly $\Lambda_{\mathbf{0}}$ when $\boldsymbol{\delta}=\mathbf{0}$. Therefore for $\boldsymbol{\delta}=\mathbf{0}$ the Hamiltonian (2.4) does not include quadratic terms in z_j.

2.3 Symmetry group of the normal forms

The Takens normal form has symmetries determined by Γ. For a fixed Γ, let us consider the group G of all linear transformations which leave every resonant monomial invariant. Since resonant monomials are $\Lambda_{\mathbf{0}}$ invariant, $\Lambda_{\mathbf{0}}^j$ with $j\in\mathbb{Z}$ obviously belong to this group. It is relatively straightforward to check that all elements of G have the form

$$(z_1,z_2,\bar z_1,\bar z_2)\mapsto(\mu_1 z_1,\mu_2 z_2,\bar\mu_1\bar z_1,\bar\mu_2\bar z_2)$$

where $(\mu_1,\mu_2)\in\mathcal{T}$. Therefore we can consider G as a (multiplicative) subgroup of the torus $\mathcal{T}$:

$$G=\{(\mu_1,\mu_2)\in\mathcal{T}:\mu_1^{k_1}\mu_2^{k_2}=1\quad\text{for all }(k_1,k_2)\in\Gamma\,\}.$$

Then for different types of resonances we have the following:

1. In the non-resonant case $G=\mathcal{T}$.
2. In the case of a simple resonance, there are two sub-cases which follow the sub-cases described in Section 2.1:
   (a) $G=\{\,(\lambda_1^j,\mu):0\leq j<q,|\mu|=1\,\}$ is a union of q circles (assuming $\alpha_1=\frac{p}{q}$ is an irreducible fraction).
   (b) G is isomorphic to a circle.

3. In the case of a double resonance G is discrete and contains $\mathrm{lcm}(q_1, q_2)$ elements:
$$G = \{\, (\lambda_1^j, \lambda_2^j) : \quad 0 \le j < \mathrm{lcm}(q_1, q_2) \,\} \,.$$

Noether's theorem implies that the normal form is integrable in the cases 1 and 2. In the case of a double resonance the symmetry group is discrete and therefore does not lead to integrability.

We also note that the Takens normal form is determined by its symmetries and different eigenvalues can lead to the same normal form. Indeed, if a pair of eigenvalues $(\tilde\lambda_1, \tilde\lambda_2)$ defines the same symmetry group as (λ_1, λ_2), the corresponding normal forms coincide. Since both (λ_1, λ_2) and $(\tilde\lambda_1, \tilde\lambda_2)$ belong to G, the total number of different pairs of eigenvalues, which lead to the same normal form is less than the number of elements in the symmetry group, $|G| = \mathrm{lcm}(q_1, q_2)$. Moreover, there is a simple relation between these eigenvalues:

$$\tilde\lambda_1 = \lambda_1^j, \quad \tilde\lambda_2 = \lambda_2^j \qquad \text{and} \qquad \lambda_1 = \tilde\lambda_1^l, \quad \lambda_2 = \tilde\lambda_2^l \,,$$

for some integer numbers j, l.

3 Arithmetic properties of the double resonances

3.1 Minimal generators

In this section we will prove a simple statement from group theory which implies that the primary resonances (two independent resonances of the lowest order) generate the whole resonance lattice.

For a point $\mathbf{r} = (k_1, k_2, \dots, k_n) \in \mathbb{Z}^n$ we define its norm by $|\mathbf{r}| = |k_1| + |k_2| + \cdots + |k_n|$. Note that for a resonance this norm coincides with its order.

Let Γ be a non-trivial subgroup of $\mathbb{Z}^n$ isomorphic to $\mathbb{Z}^2$. Let $\mathbf{r}_0 = (k_1, \dots, k_n)$ be one of the smallest (maybe non-unique, see Section 3.4) non-trivial elements of Γ and let $\mathbf{r}_1 = (m_1, \dots, m_n)$ be any of the smallest elements independent from $\mathbf{r}_0$. We say that Γ is generated by the pair $\mathbf{r}_0$ and $\mathbf{r}_1$ if any element of Γ can be represented as a linear combination of $\mathbf{r}_0$ and $\mathbf{r}_1$ with integer coefficients. If $\mathbf{r}_0$, $\mathbf{r}_1$ generate Γ we call them *minimal generators.*

Lemma 3.1. *Γ is generated by $\mathbf{r}_0$ and $\mathbf{r}_1$ always except for the case when $|\mathbf{r}_0| = |\mathbf{r}_1|$ is even and $k_j m_j = 0$ for all $j \in \{1, 2, \dots, n\}$.*

Proof. Suppose that $\mathbf{r}_0$ and $\mathbf{r}_1$ do not generate Γ. Then there is an element in Γ which cannot be represented as a linear combination of $\mathbf{r}_0$ and $\mathbf{r}_1$ with integer coefficients. Subtracting integer multiples of $\mathbf{r}_0$ and $\mathbf{r}_1$ from this element, we can find a non-trivial element $\mathbf{r}_2 \in \Gamma$ such that

$$\mathbf{r}_2 = s_0\mathbf{r}_0 + s_1\mathbf{r}_1$$

with $|s_0|, |s_1| \le \frac{1}{2}$. Then we get

$$|\mathbf{r}_2| \le |s_0|\,|\mathbf{r}_0| + |s_1|\,|\mathbf{r}_1| \le \frac{1}{2}\,(|\mathbf{r}_0| + |\mathbf{r}_1|) \le |\mathbf{r}_1|\,.$$

The last of the inequalities follows from $|\mathbf{r}_1| \ge |\mathbf{r}_0|$. On the other hand $|\mathbf{r}_2| \ge |\mathbf{r}_1|$. Therefore in the formula all non-strict inequalities should be exact equalities and we conclude that

$$|\mathbf{r}_2| = |\mathbf{r}_0| = |\mathbf{r}_1| \qquad \text{and} \qquad |s_0| = |s_1| = \frac{1}{2}\,.$$

Consequently,

$$\mathbf{r}_2^{\pm} = \frac{\mathbf{r}_0 \pm \mathbf{r}_1}{2}$$

belong to Γ and, by the arguments above, have the same norm as $\mathbf{r}_0$ and $\mathbf{r}_1$. In particular we get $|\mathbf{r}_0 + \mathbf{r}_1| = |\mathbf{r}_0| + |\mathbf{r}_1|$ or equivalently

$$|k_1 + m_1| + \cdots + |k_n + m_n| = |k_1| + \cdots + |k_n| + |m_1| + \cdots + |m_n|\,.$$

The equality is achieved if and only if $k_j m_j \ge 0$ for all j. In a similar way $|\mathbf{r}_0 - \mathbf{r}_1| = |\mathbf{r}_0| + |\mathbf{r}_1|$ implies $k_j m_j \le 0$ for all j. Combining these two inequalities we see $k_j m_j = 0$ for all j. But this case is explicitly excluded by the assumptions of the lemma. Therefore $\mathbf{r}_0$ and $\mathbf{r}_1$ generate Γ. □

We note that, for a double resonance in a $4D$ symplectic map, the group of resonances defined by (2.1) automatically satisfies the assumptions of Lemma 3.1 unless $\alpha_1 = \alpha_2 = \frac{1}{2}$. Indeed, the assumptions of the lemma are not satisfied only if $\mathbf{r}_0 = (k_1, 0)$ and $\mathbf{r}_1 = (0, k_1)$ for some integer k_1. Then

$$k_1\alpha_1 = k_3 \qquad \text{and} \qquad k_1\alpha_2 = m_3 \qquad \text{for some } k_3, m_3 \in \mathbb{Z}\,.$$

Therefore

$$\alpha_1 = \frac{k_3}{k_1}\,, \qquad \alpha_2 = \frac{m_3}{k_1}\,.$$

Then $\mathbf{r} = (m_3, -k_3)$ is obviously resonant as $m_3\alpha_1 - k_3\alpha_2 = 0$. Taking into account that $|k_3| + |m_3| = |\mathbf{r}| \ge |\mathbf{r}_0| = |k_1|$ and $0 \le \alpha_1, \alpha_2 \le \frac{1}{2}$, we see that $|k_3| = |m_3| = \frac{1}{2}|k_1|$ and therefore $\alpha_1 = \alpha_2 = \frac{1}{2}$.

The following example shows that in a higher dimension Γ is not necessarily generated by two minimal independent elements.

Example: Let $n = 3$, $\alpha_1 = \frac{1}{\sqrt{17}}$, $\alpha_2 = \frac{1}{4}$, $\alpha_3 = \frac{1}{2} - \frac{1}{\sqrt{17}}$. There are three resonances of order 4:

$$\mathbf{r}_0 = (0, 4, 0), \qquad \mathbf{r}_1 = (2, 0, 2), \qquad \mathbf{r}_2 = (1, 2, 1),$$

and it is easy to see that there are no resonances of order less than 4. So this is a double resonance of order 4.

Moreover $\mathbf{r}_0, \mathbf{r}_1$ do not generate Γ since $\mathbf{r}_2 = \frac{1}{2}(\mathbf{r}_0 + \mathbf{r}_1)$, which is obviously not a linear combination with integer coefficients. On the other hand, Lemma 3.1 implies that $\mathbf{r}_0$, $\mathbf{r}_2$ are minimal generators (as well as $\mathbf{r}_1$, $\mathbf{r}_2$).

Note that this phenomenon can happen in symplectic maps of dimension 6 or higher only. On the other hand, it does not happen in nearly integrable Hamiltonian flows in any dimension, since in that case the resonance condition takes the form $k_1\omega_1 + \cdots + k_n\omega_n = 0$ in the traditional sense and not mod 1.

3.2 Doubly strong resonances

In the study of the dynamics, the resonances of the lowest orders are of special interest. Our assumptions on the eigenvalues λ_1, λ_2 exclude resonances of orders one and two, and therefore we are left with resonances of order 3 or higher. The next lemma provides the complete list of the cases where the normal form contains at least two independent resonant terms of orders 3 or 4. In these cases we cannot consider the normal form to be a small perturbation of an integrable system, and our preliminary numerical experiments suggest that they are indeed chaotic.[1]

Note that listing the cases we assume that $0 < \alpha_1 < \alpha_2 < \frac{1}{2}$ which does not restrict the generality.

Lemma 3.2. *If the minimal generators of Γ have the orders $n_0, n_1 \in \{3, 4\}$ then the corresponding exponents (α_1, α_2) belong to the list shown in Table 1.*

[1] In the case $n_0 = 3, n_1 = 4$ the terms of order 3 do not confine the motion in a small neighbourhood of the origin. Therefore the majority of trajectories leave a small neighbourhood of the origin and reach a region where higher order terms of the normal form have a non-negligible contribution. In general, there is no reason to think that in this larger region the truncated normal form provides an accurate description for the dynamics. On the other hand, we note that the normal form truncated at order four may posses confined dynamics. The fourth order resonant terms are expected to break down the integrability of the normal form. In this sense this case should be treated as "immediately" non-integrable.

num.	α_1	α_2	n_0	n_1	3 resonances	4 resonances
1	$\frac{1}{6}$	$\frac{1}{3}$	3	3	$(2,-1)$ $(0,3)$	$(2,2)$
2	$\frac{1}{5}$	$\frac{2}{5}$	3	3	$(2,-1)$ $(1,2)$	$(3,1)$ $(1,-3)$
3	$\frac{1}{12}$	$\frac{1}{4}$	4	4	—	$(3,-1)$ $(0,4)$
4	$\frac{1}{10}$	$\frac{3}{10}$	4	4	—	$(3,-1)$ $(1,3)$
5	$\frac{1}{8}$	$\frac{3}{8}$	4	4	—	$(1,-3)$ $(3,-1)$ $(2,2)$
6	$\frac{1}{4}$	$\frac{5}{12}$	4	4	—	$(1,-3)$ $(4,0)$
7	$\frac{1}{4}$	$\frac{1}{3}$	3	4	$(0,3)$	$(4,0)$
8	$\frac{1}{9}$	$\frac{1}{3}$	3	4	$(0,3)$	$(3,-1)$
9	$\frac{2}{9}$	$\frac{1}{3}$	3	4	$(0,3)$	$(3,1)$
10	$\frac{1}{3}$	$\frac{4}{9}$	3	4	$(3,0)$	$(1,-3)$
11	$\frac{1}{8}$	$\frac{1}{4}$	3	4	$(2,-1)$	$(0,4)$
12	$\frac{1}{4}$	$\frac{3}{8}$	3	4	$(1,2)$	$(4,0)$
13	$\frac{1}{7}$	$\frac{2}{7}$	3	4	$(2,-1)$	$(1,3)$
14	$\frac{1}{7}$	$\frac{3}{7}$	3	4	$(1,2)$	$(3,-1)$
15	$\frac{2}{7}$	$\frac{3}{7}$	3	4	$(2,1)$	$(1,-3)$

Table 1: Doubly strong resonances with simple eigenvalues

We have also checked the list by running a simple computer code to ensure that no case has been missed.

Proof. The lemma is proved by solving (with respect to α_1, α_2) all possible pairs of resonant relations of orders 3 and 4. All relevant resonant lines are shown on Fig. 2.

In order to reduce the number of variants to consider, we note that if $(k_1, k_2) \in \Gamma$ then $(-k_1, -k_2) \in \Gamma$, so without loss in generality it can be assumed that in a resonance relation $k_1 \geq 0$ (and $k_2 > 0$ if $k_1 = 0$). Then a resonant term of order n must satisfy one of the conditions

$$(n-j)\alpha_1 = k_3 \pm j\alpha_2 \qquad \text{for } |k_3| = \{0, \ldots, [n/2]\},\ j = 0, \ldots, n.$$

Let us consider first the case $n_0 = n_1 = 3$. It is enough to consider 5 resonant equations: (i) $2\alpha_1 = \alpha_2$, (ii) $2\alpha_1 = 1 - \alpha_2$, (iii) $\alpha_1 = 1 - 2\alpha_2$, (iv) $3\alpha_1 = 1$

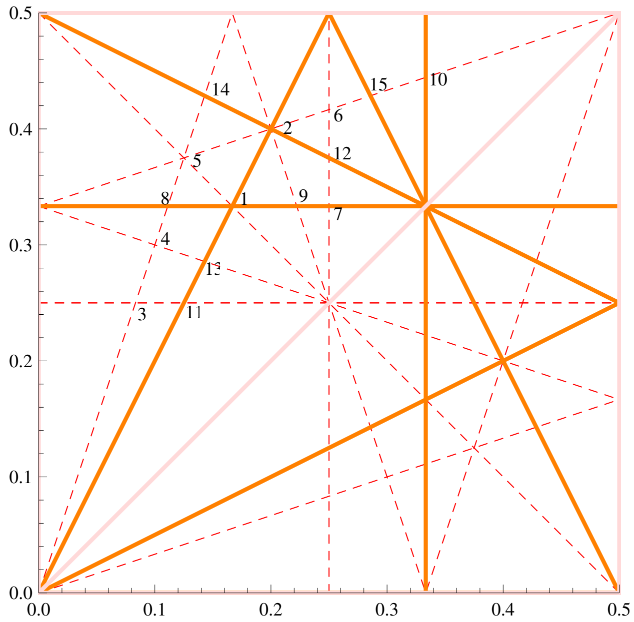

Figure 2: Graphical representation of the resonant lines of the order 3 (continuous lines) and order 4 (discontinuous lines).

and (v) $3\alpha_2 = 1$. The (i)–(iii) pair gives $(\alpha_1, \alpha_2) = (1/5, 2/5)$ and the (i)–(v) pair gives $(\alpha_1, \alpha_2) = (1/6, 1/3)$. Other pairs give no solution.

Consider the case $n_0 = n_1 = 4$. Similarly to the above case it is enough to consider 7 resonant equations: (i) $\alpha_1 = -1 + 3\alpha_2$, (ii) $4\alpha_2 = 1$, (iii) $3\alpha_1 = \alpha_2$, (iv) $4\alpha_1 = 1$, (v) $3\alpha_1 = 1 - \alpha_2$, (vi) $2\alpha_1 = 1 - 2\alpha_2$ and (vii) $\alpha_1 = 1 - 3\alpha_2$. Pairs (i)–(iii),(i)-(vi) and (iii)–(vi) give $(\alpha_1, \alpha_2) = (1/8, 3/8)$, pair (i)–(iv) gives $(\alpha_1, \alpha_2) = (1/4, 5/12)$, pair (ii)–(iii) gives $(\alpha_1, \alpha_2) = (1/12, 1/4)$ and pair (iii)–(vii) gives $(\alpha_1, \alpha_2) = (1/10, 3/10)$. Other pairs give no solution.

The case $n_0 = 3$, $n_1 = 4$ is discussed in a similar way. □

Remark 3.3. *Table 1 lists 15 cases, but the number of essentially different normal forms is only 9. Some of the double strong resonances lead to normal forms which differ by an elementary change of variables (e.g.* $(z_1, z_2) \mapsto (z_2, z_1)$*,* $(z_1, z_2) \mapsto (-\bar{z}_1, z_2)$ *or* $(z_1, z_2) \mapsto (z_1, -\bar{z}_2)$*). In particular, we can group together rows 3 and 6; 8 and 9 and 10; 11 and 12; 13 and 14 and 15 as they respectively correspond to similar normal forms. Note that the changes* $(z_1, z_2) \mapsto (-\bar{z}_1, z_2)$ *and* $(z_1, z_2) \mapsto (z_1, -\bar{z}_2)$ *are not symplectic, which should be taken into account in interpretations of this remark.*

3.3 Resonant lattices

In this section we give a more detailed description of Γ in the case of a double resonance. Let $\alpha_1 = \frac{p_1}{q_1}$, $\alpha_2 = \frac{p_2}{q_2}$. Without loss in generality we may assume that $\gcd(p_1, q_1) = 1$ and $\gcd(p_2, q_2) = 1$, *i.e.*, the greatest common factor is 1 or, in other words, α_1, α_2 are irreducible fractions.

Let $\gcd(q_1, q_2) = Q$ and define $Q_1 = q_1/Q$, $Q_2 = q_2/Q$.

Lemma 3.4. *There is a matrix* $\mathrm{A} \in \mathrm{SL}(2, \mathbb{Z})$ *such that all resonances can be represented in the form*

$$\begin{pmatrix} k_1 \\ k_2 \end{pmatrix} = \begin{pmatrix} Q_1 & 0 \\ 0 & Q_2 \end{pmatrix} \mathrm{A} \begin{pmatrix} Q & 0 \\ 0 & 1 \end{pmatrix} \begin{pmatrix} l_1 \\ l_2 \end{pmatrix}$$

where (l_1, l_2) *runs over* $\mathbb{Z}^2$.

Proof. We recall that $(k_1, k_2) \in \Gamma$ if it satisfies the equation

$$\alpha_1 k_1 + \alpha_2 k_2 = k_3$$

for some $k_3 \in \mathbb{Z}$. Let $\gcd(p_1, p_2) = P$ and define $p_1 = PP_1$, $p_2 = PP_2$. Then the resonant equation takes the form

$$\frac{P_1 P}{Q_1 Q} k_1 + \frac{P_2 P}{Q_2 Q} k_2 = k_3 \, .$$

Since $\gcd(P, Q) = \gcd(P, Q_1) = \gcd(P, Q_2) = 1$, we have $k_3 = 0 \pmod P$, i.e., there is l_1 such that $k_3 = Pl_1$. Canceling P and multiplying by Q we get

$$\frac{P_1}{Q_1} k_1 + \frac{P_2}{Q_2} k_2 = Q l_1 \, .$$

Since $\gcd(P_1, Q_1) = \gcd(P_2, Q_2) = \gcd(Q_1, Q_2) = 1$ we conclude $k_1 = 0 \pmod{Q_1}$ and $k_2 = 0 \pmod{Q_2}$. Then there are $j_1, j_2 \in \mathbb{Z}$ such that $k_1 = Q_1 j_1$ and $k_2 = Q_2 j_2$ and we obtain

$$P_1 j_1 + P_2 j_2 = Q l_1 \, . \tag{3.1}$$

Since $\gcd(P_1, P_2) = 1$ the equation $P_1 j_1^* + P_2 j_2^* = 1$ has a Euclidean solution. Then the general solution of equation (3.1) is a sum of its partial solution and a general solution of the corresponding homogeneous equation:

$$\begin{pmatrix} j_1 \\ j_2 \end{pmatrix} = \begin{pmatrix} j_1^* \\ j_2^* \end{pmatrix} Q l_1 + \begin{pmatrix} -P_2 \\ P_1 \end{pmatrix} l_2 \, .$$

Let

$$\mathrm{A} := \begin{pmatrix} j_1^* & -P_2 \\ j_2^* & P_1 \end{pmatrix} \, .$$

The definition of j_k^* implies $\det \mathrm{A} = 1$ and the lemma follows immediately. □

Corollary 3.5. *There are two basic resonances such that any other resonance is a linear combination (with coefficients from $\mathbb{Z}$) of these two. (Indeed, obviously $(l_1, l_2) = l_1(1,0) + l_2(0,1)$, then apply the lemma. We note that these two basic resonances are not necessary of the lowest orders.)*

Corollary 3.6. *If (k_1, k_2) is resonant, then $k_1 = 0 \pmod{Q_1}$ and $k_2 = 0 \pmod{Q_2}$.*

Corollary 3.7. *The points (k_1, k_2) with $k_1 = 0 \pmod{q_1}$ and $k_2 = 0 \pmod{q_2}$ are resonances. Moreover, inside the rectangle $(0, q_1) \times (0, q_2)$ there are exactly $Q - 1$ resonances. Inside this rectangle for each $k_1 = 0 \pmod{Q_1}$ there is exactly one $k_2 = 0 \pmod{Q_2}$ such that (k_1, k_2) is a resonance, and for each such k_2 exactly one such k_1. (Indeed, $\det \mathrm{A} = 1$ and the statement follows by comparison of the areas on (j_1, j_2) and (l_1, l_2) planes.)*

Corollary 3.8. *If q_1 and q_2 are mutually prime, the resonances form the rectangular lattice generated by the vectors $(q_1, 0)$ and $(0, q_2)$. (Indeed, in this case $Q = 1$ and all resonances have the form $(q_1 l_1, q_2 l_2)$ where $l_1, l_2 \in \mathbb{Z}$.)*

Lemma 3.4 implies that the area of a fundamental parallelogram of the lattice Γ equals to $QQ_1Q_2 = \mathrm{lcm}(q_1, q_2)$. As a result we get a useful tool which allows us to check if a given pair of resonances generates all the others:

Corollary 3.9. *Two elements (k_1, k_2), $(m_1, m_2) \in \Gamma$ generate Γ if and only if*

$$\det \begin{vmatrix} k_1 & k_2 \\ m_1 & m_2 \end{vmatrix} = \pm \,\mathrm{lcm}(q_1, q_2)\,. \tag{3.2}$$

3.4 Non-uniqueness of the minimal generators

The case 5 of Table 1 clearly shows that the minimal generators are not necessarily unique. The non-uniqueness has a trivial and inevitable component as $(k_1, k_2) \in \Gamma$ obviously implies $(-k_1, -k_2) \in \Gamma$. On the other hand, the corresponding terms in the complex version of a real normal form are complex conjugates and therefore can be grouped together in a natural way. In order to avoid discussing the non-uniqueness which arises from this trivial symmetry, we assume that $k_1 \geq 0$ (and $k_2 > 0$ if $k_1 = 0$). These resonances form a subset $\Gamma_+ \subset \Gamma$. Under this assumption, the minimal generators are unique for the majority of (but not for all) resonances.

Let us discuss briefly cases when the non-trivial non-uniqueness arises as in these cases the normal form has special properties.

Let $\mathbf{r}_0$ and $\mathbf{r}_1$ be minimal generators of the group of resonances Γ and let $n_k = |\mathbf{r}_k|$, $n_0 \leq n_1$. First let us discuss the case $n_1 = n_0$.

Lemma 3.10. *There are at most three pairwise independent* $\mathbf{r}_1, \mathbf{r}_2, \mathbf{r}_3 \in \Gamma_+$ *such that* $|\mathbf{r}_1| = |\mathbf{r}_2| = |\mathbf{r}_3| = n_0$*. Moreover, if there are exactly three such vectors, then* n_0 *is even, one of the resonances has the form* $(\frac{n_0}{2}, \pm\frac{n_0}{2})$*, and*

$$\alpha_1 = \frac{p_1}{q}, \qquad \alpha_2 = \frac{p_2}{q} \qquad \text{where} \quad q = \frac{n_0^2}{2}. \tag{3.3}$$

Proof. If there are more than two pairwise independent resonances with $|\mathbf{r}| = n_0$ then at least two of them are on the same side of the square $S = \{\, |\mathbf{r}| = n_0 \,\}$. Without loosing in generality let us assume that $\mathbf{r}_1$,$\mathbf{r}_2$ are in the first quadrant. Since there are no resonances of order less than n_0, the set $S_k^\pm = \{\, \mathbf{r} : |\mathbf{r} \pm \mathbf{r}_k| < n_0 \,\}$ does not contain any other resonance except for $\pm\mathbf{r}_k$ at its centre. It is not hard to see that $S \setminus \left(S_1^+ \cup S_2^+ \cup S_1^- \cup S_2^-\right)$ consists of two points only, namely, $\pm(\frac{n_0}{2}, -\frac{n_0}{2})$. If this point is resonant we get the third resonance $\mathbf{r}_3$ and, since components of $\mathbf{r}_3$ are integer, n_0 is necessarily even. Otherwise there are no more resonances of order n_0.

Now let $\mathbf{r}_1, \mathbf{r}_2, \mathbf{r}_3$ be resonant with $\mathbf{r}_3 = (\frac{n_0}{2}, -\frac{n_0}{2})$. Corollary 3.6 implies that $\frac{n_0}{2} = 0 \pmod{Q_1}$ and $\frac{n_0}{2} = 0 \pmod{Q_2}$. Since $\gcd(Q_1, Q_2) = 1$ we get $\frac{n_0}{2} = 0 \pmod{Q_2 Q_1}$. Let $\mathbf{r}_1 = (k_1, k_2)$. Since $k_1 = 0 \pmod{Q_1}$, $k_2 = 0 \pmod{Q_2}$ and $k_1 + k_2 = n_0$ we conclude $k_1 = k_2 = 0 \pmod{Q_2 Q_1}$. Lemma 3.1 implies that $\mathbf{r}_1$ and $\mathbf{r}_3$ generate Γ. Consequently, any element $\mathbf{r}$ of Γ is a combination of the minimal generators with integer coefficients, and therefore its coordinates are both divisible by $Q_1 Q_2$. Corollary 3.7 implies that the first component of $\mathbf{r}$ can have any residue when divided by Q_2 and the second component can have any residue when divided by Q_1, since those residues are always zero, we conclude $Q_1 = Q_2 = 1$, i.e., $q_1 = q_2$.

Finally, Corollary 3.9 implies that

$$\operatorname{lcm}(q_1, q_2) = \det \begin{vmatrix} \frac{n_0}{2} & k_1 \\ -\frac{n_0}{2} & k_2 \end{vmatrix} = \det \begin{vmatrix} \frac{n_0}{2} & k_1 \\ -\frac{n_0}{2} & n_0 - k_1 \end{vmatrix} = \frac{n_0^2}{2}\,.$$

Taking into account that $q_1 = q_2$ we get (3.3). $\square$

If the assumptions of Lemma 3.10 are satisfied, the minimal generators are not unique since Lemma 3.1 implies that each of the pairs $\{\mathbf{r}_1, \mathbf{r}_2\}$, $\{\mathbf{r}_2, \mathbf{r}_3\}$ or $\{\mathbf{r}_1, \mathbf{r}_3\}$ generates Γ (the number 5 of Table 1 is an example). We also note that all frequencies of the form (3.3) with $n_0 \le 70$ (a total number of 50155 resonances) either lead to the non-uniqueness of the minimal generators or are not doubly resonant of order n_0 (i.e. there is a resonance of a lower order). We do not know if this is true for all n_0.

The non-uniqueness at the leading order n_0 is a relatively rare phenomenon as it requires the frequencies to be of the special form (3.3). Indeed, Lemma 3.10 implies that if $n_0 = n_1$ but α_k do not satisfy (3.3), then there are only two (four if you take into account the trivial symmetry) resonances of the minimal order n_0. Then the minimal generators are unique (modulo the trivial symmetry $\mathbf{r} \mapsto -\mathbf{r}$).

If $n_0 < n_1$ there is exactly one resonance of order n_0 and the non-uniqueness of minimal generators can appear due to the presence of two or more pairwise independent resonances of order n_1. It is relatively easy to establish that in this case necessarily n_0 is even and $\gcd(q_1, q_2)^2 \geq \operatorname{lcm}(q_1, q_2)$ which is not satisfied by the "majority" of the frequencies.

Example ($n_0 = 4$, $n_1 = 5$): $\alpha_1 = \frac{1}{11}$, $\alpha_2 = \frac{4}{11}$. The lowest order resonance $(1, -3)$ is of order 4. There are two resonances of order 5:

$$(4, -1) \qquad (3, 2)\,.$$

Example ($n_0 = 4$, $n_1 = 5$): $\alpha_1 = \frac{1}{5}$, $\alpha_2 = \frac{3}{10}$. The lowest order resonance $(2, 2)$ is of order 4. There are three resonances of order 5:

$$(5, 0) \qquad (3, -2) \qquad (1, -4)\,.$$

Example ($n_0 = 4$, $n_1 = 7$): $\alpha_1 = \frac{1}{7}$, $\alpha_2 = \frac{5}{14}$. The lowest order resonance $(2, 2)$ is of order 4. There are four resonances of order 7:

$$(7, 0) \qquad (5, -2) \qquad (3, -4) \qquad (1, -6)\,.$$

Example ($n_0 = 4$, $n_1 = 11$): $\alpha_1 = \frac{1}{11}$, $\alpha_2 = \frac{9}{22}$. The lowest order resonance $(2, 2)$ is of order 4, there is a resonance $(4, 4)$ of order 8. There are six resonances of order 11 of the form $(11 - 2j, 2j)$ with $j \in \{\,0, 1, 2, 3, 4, 5\,\}$.

We have no doubts that this series of examples can be continued and the normal form may have any number of independent terms at the order n_1 (of course, for a large and suitably chosen n_1).

3.5 Classification by primary resonances

Consider a family $F_{\boldsymbol{\delta}}$, $\boldsymbol{\delta} = (\delta_1, \delta_2)$, of $4D$ symplectic maps such that $F_{\boldsymbol{\delta}}(\mathbf{0}) = \mathbf{0}$ and $\mathrm{Spec} DF_{\boldsymbol{\delta}}(\mathbf{0}) = \{\lambda_1, \lambda_2, \bar\lambda_1, \bar\lambda_2\}$, where $\lambda_k = \exp(2\pi i \alpha_k)$ with $\alpha_k = p_k/q_k + \delta_k$ for $k = 1, 2$. Hence for $\boldsymbol{\delta} = \mathbf{0}$ the origin is a doubly resonant fixed point. Let $\mathbf{r}_0$ and $\mathbf{r}_1$ be minimal generators of the group of resonances Γ described in Section 3.1, related to the double resonance at $\boldsymbol{\delta} = \mathbf{0}$.

It is convenient to classify the double resonances according to the order of the primary resonances. Let $n_k = |\mathbf{r}_k|$, $k = 0, 1$. We note that if $n_0 < n_1$, the normal form truncated at the order $n_1 - 1$ has the same symmetries as in the case of a simple resonance. Therefore the truncated normal form is integrable. In this case the normal form truncated at any higher order can be treated as a small perturbation of an integrable system. In addition we need to compare the contribution of these terms with the terms coming from the unavoidable resonances (which contribute to the orders 4 and higher when $\boldsymbol{\delta} = \mathbf{0}$). If $n_0 \geq 5$ the fixed point is called *weakly resonant* and otherwise it will be called *strongly resonant*. In the weakly resonant case the dynamics generically can be considered as a small perturbation of a non-resonant normal form.

Let us list the principal cases:

1. Weak double resonances:

   (a) $5 \leq n_0 < n_1$: up to the order $n_0 - 1$ the normal form looks like the normal form of a non-resonant fixed point. The resonant terms of order from n_0 to $n_1 - 1$ provide an *integrable* perturbation. Finally, including the terms of order n_1, one expects (in general) to get a non-integrable system. In a non-degenerate case, Nekhoroshev theory implies stability of the fixed point on exponentially long times [1, 2].

   (b) $5 \leq n_0 = n_1$: up to the order $n_0 - 1$ the normal form looks like the normal form of a non-resonant fixed point. After adding the resonant terms of order n_0 we expect (in general) to get a non-integrable system. In a non-degenerate case, the stability properties are the same as above.

2. Simply strong double resonances: $n_0 \leq 4 < n_1$: up to the order $n_1 - 1$ the normal form looks like a family of strongly resonant integrable systems (similar to the case of a two dimensional map). Then including the terms of order n_1 we expect in general to get a non-integrable system.

3. Doubly strong double resonances (Table 1 shows the complete list):

   (a) $n_0 = n_1 = 3$: generically the leading order of the normal form is not integrable and does not confine dynamics.[2]

[2] If $n_0 = n_1 \leq 4$, the leading order is a homogeneous vector field for $\boldsymbol{\delta} = \mathbf{0}$, which implies that the dynamics in all energy levels is essentially the same. Note that this paper does not include any proof for non-integrability of the leading order of the normal form, although we think this to be true.

(b) $n_0 = 3$, $n_1 = 4$: generically the leading order of the normal form is integrable but it does not confine dynamics.

(c) $n_0 = n_1 = 4$: generically the leading order of the normal form is not integrable. The dynamics may be confined (or not confined) in a small neighbourhood of the fixed point depending on the values of the coefficients in the normal form.

We note that if the leading order of the normal form does not confine the dynamics, it is possible to take into account terms of higher order to get confined dynamics. Unfortunately, this procedure will typically confine dynamics in a region which is noticeably larger than the domain of validity of the normal form theory and, consequently, the dynamics of the normal form on that large invariant set may substantially differ from the dynamics of the original map.

4 Non-integrability of a weak resonance

Let $F_{\boldsymbol{\delta}}$ be a family of $4D$ symplectic maps having for $\boldsymbol{\delta} = \mathbf{0}$ the origin as a doubly resonant fixed point. The normal form of $F_{\boldsymbol{\delta}}$ near the double resonance (i.e. for $0 < \delta << 1$ small, $\delta = \|\boldsymbol{\delta}\|$) is described by a Hamiltonian with two degrees of freedom. In this section we establish non-integrability of a generic truncated normal form which corresponds to the case 1(a) of Section 3.5. Instead of studying the normal form in its full generality, we will perform the analysis of a truncated model introduced in [11], the general case being a small perturbation of this model. It is important to note that in our case the validity of the model requires that $n_1 > n_0$ (meanwhile in [11] it was necessary to assume $n_1 \gg n_0$).

Let (k_1, k_2) and (m_1, m_2) be minimal generators of Γ. Without loosing in generality, we assume $k_1, m_1 \geq 0$. In the following, we consider the minimal generators to be unique in the sense of Section 3.4 since this is the most common case. In the following we rescale (and truncate) the normal form to obtain a suitable model describing the dynamics at the junction of two resonances. The dependence of the truncated model, see equation (4.1), on the angles is given explicitly by periodic (cosinus) functions. In the case of non-unique minimal generators, a trigonometric polynomial replaces $\cos(\psi_2)$.

It is convenient to define

$$\begin{array}{rclcrcl} \psi_1 & = & k_1\varphi_1 + k_2\varphi_2, & \qquad & \psi_2 & = & m_1\varphi_1 + m_2\varphi_2, \\ I_1 & = & k_1 J_1 + m_1 J_2, & & I_2 & = & k_2 J_1 + m_2 J_2\,. \end{array}$$

It is easy to check that this change of variables is symplectic.

On the other hand the Jacobian of the change $(\varphi_1, \varphi_2) \mapsto (\psi_1, \psi_2)$ is given by (3.2). It is integer and larger than one. Its value depends on arithmetic properties of α_1, α_2. The normal form Hamiltonian is 2π-periodic in φ_1 and φ_2. We will see that in the new variables, the Hamiltonian function is also 2π-periodic in ψ_1 and ψ_2. Since the Jacobian of the change is larger than one, the Hamiltonian has a shorter lattice of periods on the standard torus in (φ_1, φ_2) variables. This property reflects the symmetry of the normal form.

Since (k_1, k_2) and (m_1, m_2) generate Γ we can rewrite Hamiltonian (2.3) in the form

$$H_{\boldsymbol{\delta}} = \sum_{l_1, l_2 \geq 0} I_1^{|p_1|/2} I_2^{|p_2|/2} A_{l_1 l_2}(J_1, J_2, \boldsymbol{\delta}) \cos\bigl(l_1\psi_1 + l_2\psi_2 + B_{l_1 l_2}(J_1, J_2, \boldsymbol{\delta})\bigr) ,$$

where $p_j = l_1 k_j + l_2 m_j$ for $j = 1, 2$, and the amplitudes $A_{l_1 l_2}$ and the phases $B_{l_1 l_2}$ are formal series in I_1, I_2 and $\boldsymbol{\delta}$.

Taking into account that (k_1, k_2) and (m_1, m_2) are minimal generators, the lower order terms correspond to multiples of (k_1, k_2), so the Hamiltonian has the following structure:

$$H_{\boldsymbol{\delta}} = H_0(J_1, J_2, \boldsymbol{\delta}) + H_1(J_1, J_2, \psi_1, \boldsymbol{\delta}) + H_2(J_1, J_2, \psi_1, \psi_2, \boldsymbol{\delta}) + \mathcal{O}_{n_1+1}(\boldsymbol{z}),$$

where $\boldsymbol{z} = (z_1, \bar{z}_1, z_2, \bar{z}_2)$ and

$$\begin{aligned}
H_0 &= A_{00}(J_1, J_2, \boldsymbol{\delta}) , \\
H_1 &= \sum_{l_1=1}^{n_1/n_0} I_1^{l_1|k_1|/2} I_2^{l_1|k_2|/2} A_{l_1 0}(J_1, J_2, \boldsymbol{\delta}) \cos\bigl(l_1\psi_1 + B_{l_1 0}(J_1, J_2, \boldsymbol{\delta})\bigr) , \\
H_2 &= I_1^{|m_1|/2} I_2^{|m_2|/2} A_{01}(0, 0, \boldsymbol{\delta}) \cos\bigl(\psi_2 + B_{01}(0, 0, \boldsymbol{\delta})\bigr) .
\end{aligned}$$

Obviously, the Hamiltonian functions H_0 and $H_0 + H_1$ are independent from ψ_2 and therefore they are both integrable with J_2 as an integral of motion. On the other hand, the addition of H_2 can lead to non-integrability and chaotic behaviour.

Let us consider this Hamiltonian in a δ-neighbourhood (in $\boldsymbol{z}$ coordinates) of the origin. Here $0 < \delta << 1$ stands for $\|\boldsymbol{\delta}\|$ and we use below $\delta_k = c_j \delta$, $j = 1, 2$, with suitable constants $c_j \in \mathbb{R}$, $c_1^2 + c_2^2 = 1$. We note that in this neighbourhood $J_1, J_2 = \mathcal{O}(\delta^2)$. Then we can write down the lowest order terms in H_0:

$$H_0 = c_1\delta J_1 + c_2\delta J_2 + a_1 J_1^2 + a_2 J_1 J_2 + a_3 J_2^2 + \mathcal{O}(\delta^5),$$

where c_j and a_j are some constants which can be expressed in terms of the coefficients from (2.3). Moreover $H_1 = \mathcal{O}(\delta^{n_0})$ and $H_2 = \mathcal{O}(\delta^{n_1})$. Since $n_1 > n_0$

≥ 5 we can consider $H_{\boldsymbol{\delta}}$ as a small perturbation of H_0. The phase space of H_0 is foliated into invariant tori $J_1, J_2 =$const bearing quasi-periodic motion with the frequency vector $\omega = \nabla H_0$. This vector vanishes at $J_1 = J_2 = 0$ for $\delta = 0$.

If $\Delta = a_2^2 - 4a_1a_3 \neq 0$ the implicit function theorem implies that the equation $\omega = 0$ has a solution at a point of the form $J_1 = \delta r_1$, $J_2 = \delta r_2$, which defines a torus of fixed points for the Hamiltonian system H_0. One has $r_1 = (2a_3c_1 - a_2c_2)/\Delta + \mathcal{O}(\delta)$, $r_2 = (2a_1c_2 - a_2c_1)/\Delta + \mathcal{O}(\delta)$. When we interpret this conclusion for the original system, two cases should be considered here as I_k are radial components of polar coordinates and therefore are to be positive (otherwise the found torus is not real). Therefore, *the torus of fixed points is born in the normal form of a generic one-parametric family if and only if the coefficients of the normal form satisfy* $\hat{r}_1, \hat{r}_2 > 0$, where we assume that the torus with $\omega = 0$ is given by $I_1 = \hat{r}_1\delta$, $I_2 = \hat{r}_2\delta$. We do not provide an explicit expression of $\hat{r}_1, \hat{r}_2$ in terms of the normal form coefficients here, as getting this condition is a matter of a routine computation.

We also note that in a generic two-parametric family this picture has an easy geometrical interpretation as generically the map from the space of parameters to the space of frequencies is a local diffeomorphism. On the plane of parameters the double resonance is located at an intersection of two resonant lines (like in Fig. 1). These lines define locally four sectors, the torus of fixed points corresponds to one of the sectors where both actions I_1, I_2 are positive on the torus. Note that the lines are defined by $I_1 = 0$ and $I_2 = 0$ respectively.

In order to study dynamics near the torus of fixed points we shift the origin to its position and scale the action variables and the Hamiltonian: $J_k = \delta r_k + \delta^{n_0/4}\tilde{J}_k$ and $H = \delta^{n_0/2}\tilde{H}$ (see details in [17]). We note that the translation is designed to eliminate the part linear in J_k of H_0 at all orders up to $\mathcal{O}(\delta^{n_1+1})$. Skipping the tildes for the sake of notation simplicity, we get

$$\begin{aligned} H_0(J_1, J_2, \boldsymbol{\delta}) &= a_1J_1^2 + a_2J_1J_2 + a_3J_2^2 + \mathcal{O}(\delta^{n_0/4}) \,, \\ H_1(J_1, J_2, \psi_1, \boldsymbol{\delta}) &= \sum_{l_1=1}^{n_1/n_0} \delta^{(l_1-1)n_0/2}\tilde{A}_{l_1 0}(J_1, J_2, \boldsymbol{\delta}) \cos\bigl(l_1\psi_1 + \tilde{B}_{l_1 0}(J_1, J_2, \boldsymbol{\delta})\bigr) \,, \\ H_2(J_1, J_2, \psi_1, \psi_2, \boldsymbol{\delta}) &= \delta^{(n_1-n_0)/2}a_{01}\cos\bigl(\psi_2 + b_{01}\bigr) \,. \end{aligned}$$

In particular, if additionally $n_1 < 2n_0$, only one harmonic ($l_1 = 1$) in the leading order is left and the form of the Hamiltonian can be further simplified by shifting the angles to eliminate the phases:

$$\begin{aligned} H_0(J_1, J_2, \boldsymbol{\delta}) &= a_1 J_1^2 + a_2 J_1 J_2 + a_3 J_2^2 + \delta^{n_0/4} \hat{A}_{00}(J_1, J_2, \delta)\,, \\ H_1(J_1, J_2, \psi_1, \boldsymbol{\delta}) &= \big(a_{10} + \delta^{n_0/4-1} \hat{A}_{10}(J_1, J_2, \boldsymbol{\delta})\big) \cos\psi_1\,, \\ H_2(J_1, J_2, \psi_1, \psi_2, \boldsymbol{\delta}) &= \delta^{(n_1-n_0)/2} a_{01} \cos\psi_2\,. \end{aligned} \tag{4.1}$$

We used that the substitutions produce series of $\tilde{A}_{l_1 0}(J_1, J_2, \boldsymbol{\delta})$ in powers of $\delta^{n_0/4-1} J_k$ and δ to clarify the structure of H_1. We refer to [17] for details.

4.1 Analysis of a truncated model

A good initial idea about the dynamics near an intersection of two weak resonances of different orders can be obtained from the Hamiltonian system given by the Hamiltonian function

$$H(\psi_1, \psi_2, J_1, J_2) = \frac{J_1^2}{2} + a_2 J_1 J_2 + a_3 \frac{J_2^2}{2} + \cos(\psi_1) + \epsilon\cos(\psi_2), \tag{4.2}$$

where a_2, a_3 and ϵ are real parameters. The corresponding symplectic form is $\Omega = d\psi_1 \wedge dJ_1 + d\psi_2 \wedge dJ_2$. This Hamiltonian can be considered as an example of the normal form described in the previous section. Indeed it coincides with (4.1) ignoring $\mathcal{O}(\delta^{n_0/4-1})$, hence describing the dynamics in a junction of resonances of different ($n_0 \neq n_1$) but similar order ($n_1 < 2n_0$). The analysis of the general normal form can be performed using the methods described below and we expect similar conclusions to be reached.

The (symplectic) change of coordinates $\tilde{\psi}_1 = \psi_1$, $\tilde{\psi}_2 = \psi_2 - a_2\psi_1$, $\tilde{J}_1 = J_1 + a_2 J_2$, $\tilde{J}_2 = J_2$, reduces (4.2) to

$$H(\psi_1, \psi_2, J_1, J_2) = \frac{J_1^2}{2} + d\frac{J_2^2}{2} + \cos(\psi_1) + \epsilon\cos(\psi_2 + a_2\psi_1), \tag{4.3}$$

where, for simplicity, we have skipped tildes and let $d = a_3 - a_2^2$. From now on we will assume $d \neq 0$. Note that (4.3) is generically not periodic but quasi-periodic in ψ_1. The new equations of motion are given by

$$\begin{aligned} &\dot{\psi}_1 = J_1, \quad \dot{J}_1 = \sin(\psi_1) + a_2\,\epsilon\sin(\psi_2 + a_2\psi_1), \\ &\dot{\psi}_2 = dJ_2, \quad \dot{J}_2 = \epsilon\sin(\psi_2 + a_2\psi_1). \end{aligned} \tag{4.4}$$

From now on we shall consider $a_2 \notin \mathbb{Z}$. The equations (4.4) have 4 fixed points: $p_1 = (0,0,0,0)$, $p_2 = (0,\pi,0,0)$, $p_3 = (\pi, -a_2\pi, 0, 0)$ and $p_4 = (\pi, (1-a_2)\pi, 0, 0)$. The character of these points depends on $\nu = \epsilon d$. Without loosing generality we consider $\nu > 0$. If $\nu < 0$ then $\psi_2 \to \psi_2 - \pi$ and $\epsilon \to -\epsilon$ reduces the system to a Hamiltonian system defined by (4.3) with $\nu > 0$. Considering $|\epsilon|$ small enough one has, for $\nu > 0$, that the point p_1 is hyperbolic-hyperbolic, p_2 is hyperbolic-elliptic, p_3 is elliptic-hyperbolic and p_4 is elliptic-elliptic.

The system (4.3) is reversible, the involutions

$$\begin{aligned} R_0(\psi_1, \psi_2, J_1, J_2) &= (2\pi - \psi_1, -2\pi a_2 - \psi_2, J_1, J_2), \\ R_1(\psi_1, \psi_2, J_1, J_2) &= (2\pi - \psi_1, 2\pi(1 - a_2) - \psi_2, J_1, J_2), \end{aligned}$$

reverse the direction of the vector field. The fixed points of the involution R_k form a plane P_k, where

$$\begin{aligned} P_0 &= \{\, \psi_1 = \pi,\ \psi_2 = -\pi a_2 \,\}, \\ P_1 &= \{\, \psi_1 = \pi,\ \psi_2 = \pi(1 - a_2) \,\}. \end{aligned}$$

We will use the reversibility to obtain stable manifolds from unstable ones. The intersection of an unstable manifold with P_k, $k = 0, 1$, consists of homoclinic points. Later in this section we establish existence of homoclinic points and study their transversality properties which are responsible for the creation of chaotic dynamics.

For $\epsilon = 0$ the variable ψ_2 is cyclic and J_2 is a first integral of motion independent of the Hamiltonian (4.3). For each value of J_2 the dynamics in the variables ψ_1, J_1 is governed by the classical pendulum Hamiltonian

$$H_1^0 = \frac{J_1^2}{2} + \cos(\psi_1)\,, \tag{4.5}$$

which is 2π-periodic in ψ_1. We note that the cylinder $\Pi_0^0 = \{\psi_1 = 0, J_1 = 0\}$ is a normally hyperbolic invariant manifold (NHIM) and the dynamics on this manifold is given by

$$\dot\psi_2 = dJ_2, \qquad \dot J_2 = 0. \tag{4.6}$$

So the cylinder Π_0^0 is foliated by periodic orbits C_h^0 which lie at the intersection of the $2D$ cylinder Π_0^0 and a $3D$ energy level $H = h$, where H refers to Hamiltonian (4.3) with $\epsilon = 0$.

The cylinder Π_0^0 has stable and unstable invariant manifolds. The unstable manifold is given explicitly as a graph

$$J_1 = 2 \sin \frac{\psi_1}{2}\,.$$

For a small $|\epsilon| > 0$, the normal hyperbolicity theory [18, 19, 20] implies the existence of a 3-dimensional NHIM close to $W^u(\Pi_0^0)$, which is an unstable manifold $W^u(\Pi^0_\epsilon)$ of an invariant cylinder Π^0_ϵ located near Π^0_0. Note that the classical theory of normal hyperbolicity is applicable to compact manifolds only. In order to satisfy this requirement we implicitly assume all consideration to be conducted in a compact invariant subset $|H| \le \text{const}$. See [21, 13] for a suitable formulation of the persistence theorems adapted to this particular case.

Since $W^u(\Pi^0_\epsilon)$ depends smoothly on ϵ and the unperturbed manifold intersects the symmetry planes P_k transversely along the line $\{\psi_1 = \pi, \psi_2 = \pi(k - a_2), J_1 = 2\}$, the implicit function theorem implies that $W^u(\Pi^0_\epsilon) \cap P_k$ contains a line close to the unperturbed one. This line consists of homoclinic points of the system (4.4). Note that, for a given value of J_2, these points belong to different levels of the energy, and they come from different orbits in the NHIM. In order to analyse transversality of the homoclinic points, we can look for $W^u(\Pi^0_\epsilon)$ in the form of a graph:

$$J_1 = 2\sin\frac{\psi_1}{2} + \epsilon f(\psi_1, \psi_2, J_2; \epsilon)\,. \tag{4.7}$$

Since this graph is invariant, the normal vector

$$\mathbf{n} = (\cos\tfrac{\psi_1}{2} + \epsilon\partial_{\psi_1} f,\ \epsilon\partial_{\psi_2} f,\ -1,\ \epsilon\partial_{J_2} f)$$

should be orthogonal to the vector field (4.4). Expanding the orthogonality condition in powers of ϵ we conclude that $f_0 = f(\psi_1, \psi_2, J_2; 0)$ must satisfy the following first order linear partial differential equation:

$$2\sin\tfrac{\psi_1}{2}\partial_{\psi_1} f_0 + \cos\tfrac{\psi_1}{2} f_0 + dJ_2\partial_{\psi_2} f_0 - a_2\sin(\psi_2 + a_2\psi_1) = 0\,.$$

Using the method of the characteristics we obtain the unique solution of this equation which is regular at $\psi_1 = 0$

$$f_0 = \frac{1}{2\sin\frac{\psi_1}{2}}\int_0^{\psi_1} g(s, \psi_2 + dJ_2\log[\tan(\tfrac{s}{4})/\tan(\tfrac{\psi_1}{4})])\,ds, \tag{4.8}$$

where $g(\psi_1, \psi_2) = a_2\sin(\psi_2 + a_2\psi_1)$. The graph representation (4.7)–(4.8) of $W^u(\Pi^0_\epsilon)$ also includes the invariant cylinder

$$\Pi^0_\epsilon = \left\{\, \psi_1 = \epsilon g_1(\psi_2, J_2),\ J_1 = \epsilon g_2(\psi_2, J_2) \,\right\},$$

which is located $\mathcal{O}(\epsilon)$-close to Π^0_0. A direct computation gives

$$g_1(\psi_2, J_2) = \frac{-a_2\sin(\psi_2)}{1 + d^2J_2^2} + \mathcal{O}(\epsilon), \qquad g_2(\psi_2, J_2) = \frac{-dJ_2a_2\cos(\psi_2)}{1 + d^2J_2^2} + \mathcal{O}(\epsilon).$$

We note that the system (4.3) also has an invariant cylinder $\Pi_\epsilon^{2\pi}$ close to $\Pi_0^{2\pi} = \{\psi_1 = 2\pi, J_1 = 0\}$, which can be obtained by application of the reversible symmetry:

$$\Pi_\epsilon^{2\pi} = R_k(\Pi_\epsilon^0)\,.$$

The same cylinder is obtained for $k = 0$ and $k = 1$. We note that the Hamiltonian (4.3) is not periodic in ψ_1, but it is obtained from the system (4.2), which is indeed periodic in both angles ψ_1 and ψ_2. In the original coordinates the cylinders Π_ϵ^0 and $\Pi_\epsilon^{2\pi}$ coincide modulus 2π in angle variables. For that reason we will use the word "homoclinic" (and not "heteroclinic") for points in $W^u(\Pi_\epsilon^0) \cap W^s(\Pi_\epsilon^{2\pi})$.

For $\epsilon = 0$, one has $W^u(\Pi_0^0) = W^s(\Pi_0^{2\pi})$. In order to study the splitting of the separatrices for $|\epsilon| > 0$ we consider the intersection of $W^u(\Pi_\epsilon^0)$ with the section $\psi_1 = \pi$. The implicit function theorem implies that this intersection is diffeomorphic to a cylinder. Moreover, (4.7) implies that the intersection is given by

$$J_1 = 2 + \epsilon f_0(\pi, \psi_2, J_2) + \mathcal{O}(\epsilon^2)\,. \tag{4.9}$$

Using (4.8) and the reversibility with respect to R_0 (or R_1) we write the difference between the stable and unstable separatrices on the section in the form

$$\begin{aligned} J_1^s - J_1^u &= \epsilon\big(f_0(\pi, -2\pi a_2 - \psi_2, J_2) - f_0(\pi, \psi_2, J_2)\big) + \mathcal{O}(\epsilon^2) \\ &= \epsilon A(J_2)\sin(\psi_2 + \pi a_2) + \mathcal{O}(\epsilon^2), \end{aligned}$$

where

$$A(J_2) = a_2 \int_0^\pi \cos\big(a_2(s-\pi) + dJ_2 \log[\tan(\tfrac{s}{4})]\big)\, ds\,. \tag{4.10}$$

The reversible symmetry implies that the difference vanishes precisely for $\psi_2 = -\pi a_2 \pmod{\pi}$, therefore the separatrices intersect along the lines

$$\begin{aligned} \ell_0 &= \{\, (\psi_1, \psi_2, J_1, J_2) : J_1 = 2 + \epsilon f(\psi_1, \psi_2, J_2; \epsilon),\ \psi_1 = \pi,\ \psi_2 = -\pi a_2 \,\} \\ \ell_1 &= \{\, (\psi_1, \psi_2, J_1, J_2) : J_1 = 2 + \epsilon f(\psi_1, \psi_2, J_2; \epsilon),\ \psi_1 = \pi,\ \psi_2 = \pi(1 - a_2) \,\}\,. \end{aligned}$$

A straightforward computation shows that the intersections are transversal provided $A(J_2) \neq 0$ and $|\epsilon| > 0$ is sufficiently small.

For $J_2 = 0$ we can compute the integral explicitly obtaining $A(0) = \sin(\pi a_2)$, and consequently the intersections are transversal in a neighbourhood of $J_2 = 0$ provided $a_2 \notin \mathbb{Z}$. For values of $J_2 > 0$, we can numerically evaluate the integral $A(J_2)$ (the change $t = \log(\tan(s/4))$ is advisable). For these purposes, we introduce $\tilde{J}_2 = dJ_2$ and we can write

$$A(J_2) = 4a_2 \int_{-\infty}^0 \cos\big(a_2(4\arctan(\exp(t)) - \pi) + \tilde{J}_2 t\big) \frac{1}{\exp(t) + \exp(-t)}\, dt\,.$$

The Fig. 3 shows the lines that the zeros of $A(J_2)$ describe in the $(a_2, \tilde{J}_2)$-plane. Note that for any weak double resonance we get some concrete values a_2 and d. Then, from the computations shown in Fig. 3 we conclude that the manifolds $W^s(\Pi_\epsilon^0)$ and $W^s(\Pi_\epsilon^{2\pi})$ intersect transversally except for some concrete values of J_2. Moreover, the numerical computations show that the lines in Fig. 3 accumulate to the set of half-integer values as $\tilde{J}_2 \to +\infty$. Hence, one has evidence that, for a fixed value of a_2, the number of zeros of $A(J_2)$ is finite. In particular for $a_2 \le 1/2$ the function $A(\tilde{J}_2)$ has no zeros.

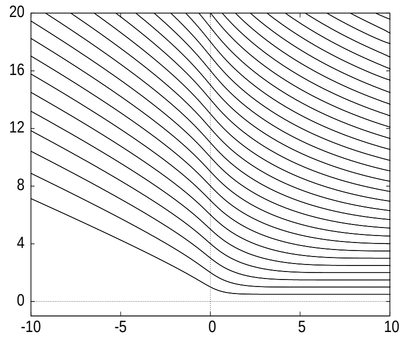

Figure 3: Set of lines for which the integral $A(J_2)$, given by (4.10), vanishes. The rescaled coordinate $\tilde{J}_2 = dJ_2$ ranges in the horizontal axis while a_2 ranges in the vertical one. See the text for details.

To compare the result of the computation of $A(J_2)$ with direct numerical results we have computed some periodic orbits on the circulation domain of the NHIM and then the corresponding manifolds and splitting. Certainly these periodic orbits have not a constant value of J_2, but the variations are only $\mathcal{O}(\epsilon)$ for finite values of J_2 (either positive of negative). For a test case, we set $d = 1$ and $a_2 = 2.75$. The plots in Fig. 4 show the value of $A(J_2)/(4a_2)$ (solid lines) and the angle between the stable and unstable manifolds at the homoclinic point $\psi_2 = -\pi a_2$ divided by $4a_2\epsilon$ for $\epsilon = 0.001$ (discontinuous lines) and $\epsilon = 0.01$ (dotted lines). Note that the value for $\epsilon = 0.001$ coincides so well with the theoretical prediction that the discontinuous lines are almost coincident with the continuous ones.

The following considerations imply that in what concerns to the homoclinic orbits the majority of the detected ones are bi-asymptotic to a periodic orbit on the cylinder, but the ones at the corresponding concrete energy value of the hyperbolic equilibrium p_1 (at the origin) are bi-asymptotic to p_1. In particular, we note that for $\epsilon = 0$ the system (4.3) has homoclinic trajectories to the point $p_2 = (0, \pi, 0, 0)$ (related to the separatrices of the pendulum (4.5)). This point becomes hyperbolic-elliptic for small $|\epsilon| > 0$ and, conse-

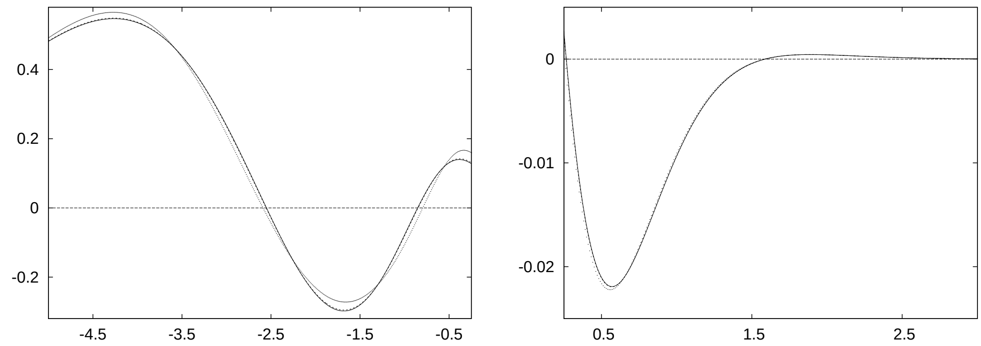

Figure 4: The theoretical splitting $J_1^s - J_2^u$ for $a = 2.75$, $d = 1$ and different ranges of J_2 and the numerically computed values for $\epsilon = 0.001$ and $\epsilon = 0.01$. See the text for details about the scaling factors and the line codes used in the plots.

quently, has one dimensional stable and unstable manifolds which are close to the unperturbed homoclinic orbit. Nevertheless, we will see that the perturbed system does not have a homoclinic orbit close to the unperturbed ones, i.e., the homoclinic connections are destroyed by the perturbation.

On the other hand, the Hamiltonian dynamics preserves energy and it is therefore important to see if the transversality of the invariant manifolds $W^u(\Pi_\epsilon^0)$ and $W^s(\Pi_\epsilon^{2\pi})$ implies existence of transversal homoclinic orbits in various energy levels.

We note that Π_ϵ^0 is a two-dimensional invariant symplectic manifold and hence the restriction of the system on this manifold is a Hamiltonian system with one degree of freedom. Such systems are integrable and therefore a complete description of the restricted dynamics is possible: the cylinder consists of domains filled with periodic orbits separated by separatrices. Indeed, $\psi_1, J_1 = \mathcal{O}(\epsilon)$ on the cylinder and the equation (4.3) implies that the restriction of H on Π_ϵ^0 is given by

$$H_{2,\epsilon}^0(\psi_2, J_2) = d\frac{J_2^2}{2} + \epsilon\cos(\psi_2) + 1 + \mathcal{O}(\epsilon^2), \tag{4.11}$$

where (ψ_2, J_2) are used as coordinates on the cylinder. Therefore, for $\epsilon = 0$ the cylinder Π_0^0 is foliated by invariant lines $J_2 = \text{const}$, all lines are periodic orbits except for the line $J_2 = 0$ which consists of equilibria. The perturbed system has on Π_ϵ^0 a $\mathcal{O}(\sqrt{\epsilon})$-small pendulum-like separatrix loop and periodic orbits inside this loop (see Fig. 5).

The cylinder Π_ϵ^0 also contains the two equilibria $p_1 = (0,0,0,0)$ and $p_2 = (0,\pi,0,0)$ of the system. Let $h_1 = H(p_1) = 1+\epsilon$ be the energy of the hyperbolic equilibrium and $h_2 = H(p_2) = 1-\epsilon$ be the energy of the hyperbolic-elliptic one. Note that h_2 is the minimal value of H on Π_ϵ^0, but this value is larger than the global minimum of H which equals to the energy $h_4 = H(p_4) = -1-\epsilon$ at the totally elliptic fixed point $p_4 = (\pi,(1-a_2)\pi,0,0)$.

The separatrix loop has the energy h_1. Let C_h^ϵ denote a periodic orbit in Π_ϵ^0 with energy h. If $h > h_1$ there are two periodic orbits with the same energy, one has $J_2 > 0$ and the other $J_2 < 0$. If $h \in (h_2, h_1)$, there is exactly one periodic orbit C_h^ϵ which crosses the axis $J_2 = 0$ twice. See Fig. 5 for a representation.

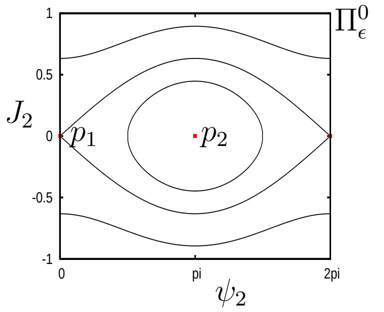

Figure 5: Sketch of the pendulum structure born at Π_ϵ^0 for $|\epsilon| > 0$. For $h > h_1$ there are two rotational curves C_h^ϵ, at $h = h1$ there is the separatrix related to p_1 and for $h_2 < h < h_1$ there is a librational curve C_h^ϵ.

Any point $\mathbf{p} \in \ell_k$ with $k = 0$ or 1 is homoclinic to the cylinder Π_ϵ^0, and, since the energy is preserved, it is homoclinic to C_h^ϵ with $h = H(\mathbf{p})$. More precisely, it belongs to $W^u(C_h^\epsilon) \cap W^s(R_k(C_h^\epsilon))$. Suppose, $W^u(\Pi_\epsilon^0)$ and $W^s(\Pi_\epsilon^{2\pi})$ intersect transversely at $\mathbf{p}$. Does it imply that the separatrices of the periodic orbit C_h^ϵ intersect transversally inside the energy level $\{\, H = h \,\}$?

In order to answer this question we note that the intersection of the tangent spaces $T_{\mathbf{p}} W^u(\Pi_\epsilon^0) \bigcap T_{\mathbf{p}} W^s(\Pi_\epsilon^{2\pi})$ is two-dimensional and can be spanned by two vectors: one is the Hamiltonian vector field $X_H(\mathbf{p})$ and the other one is a vector $v_{\mathbf{p}} \in T_{\mathbf{p}}\ell_k$, tangent to the line of homoclinic points ℓ_k. On the other hand

$$\mathbf{p} \in W^u(C_h^\epsilon) \cap W^s(R_k(C_h^\epsilon)).$$

This intersection is transversal inside the energy level iff the intersection

$$T_{\mathbf{p}} W^u(C_h^\epsilon) \cap T_{\mathbf{p}} W^s(R_k(C_h^\epsilon))$$

is one dimensional. Equivalently, it is spanned by $X_H(\mathbf{p})$ as this vector is obviously tangent to any invariant manifold. Since

$$T_{\mathbf{p}}W^u(C_h^\epsilon) \cap T_{\mathbf{p}}W^s(R_k(C_h^\epsilon)) = T_{\mathbf{p}}\{\, H = h\, \}\,,$$

the transversality condition is satisfied iff $T_{\mathbf{p}}\ell_k \notin T_{\mathbf{p}}\{\, H = h\, \}$.

We note that $T_{\mathbf{p}}\ell_k \in T_{\mathbf{p}}\{\, H = h\, \}$ iff $\mathbf{p}$ is a critical point of the Hamiltonian H restricted onto ℓ_k. Substituting (4.9) with $\psi_2 = \pi(k - a_2)$ into (4.3) we get an approximation

$$H = d\frac{J_2^2}{2} + 2\epsilon f_0(\pi, \pi(k - a_2), J_2) + 1 + (-1)^k\epsilon + \mathcal{O}(\epsilon^2)\,.$$

Consequently, the only critical point for $d > 0$ (resp. $d < 0$) is the minimum (resp. maximum) at $J_2 = \mathcal{O}(\epsilon)$. The corresponding critical values are $H = E_k$ with

$$E_k = 1 + \epsilon(-1)^k \cos \pi a_2 + \mathcal{O}(\epsilon^2).$$

Therefore if $H(\mathbf{p}) = E_k$, the transversal homoclinic orbit (considered as an intersection of the stable and unstable manifolds of the normally hyperbolic cylinder) is not transversal as an intersection inside the fixed energy level. Moreover, as E_k is the minimum (resp. maximum) of H on ℓ_k, it is obvious that $\ell_k \cap W^u(C_h^\epsilon) = \emptyset$ for $h < E_k$ (resp. $h > E_k$). Note that $h_2 < E_k < h_1$ provided that $a_2 \notin Z$ and $|\epsilon|$ is small enough.

Remark 4.1. *For the rotational invariant curves on Π_ϵ^0 one has $|h| > h_1$ and the condition $A(J_2) \neq 0$ immediately implies that the intersection between $W^u(\Pi_\epsilon^0)$ and $W^s(\Pi_\epsilon^{2\Pi})$ is transversal inside the energy level. For fixed values of a_2 and d, and according to the computations shown in Fig. 3, the intersection is transversal for negative large enough values of $\tilde{J}_2$. Transversality also holds for positive large enough values of $\tilde{J}_2$ provided $a_2 \neq k/2$, $k \in \mathbb{Z}$. Note also that (4.10) is a one-frequency oscillatory integral then, for values of $|J_2|$ large enough, one has $|A(J_2)| \leq c_1 \exp(-c_2 J_2)$.*

In particular, let us consider $h = h_1 = H(p_1) = 1 + \epsilon$. Note that this is the degenerated case: C_h^0 is a curve of fixed points and C_h^ϵ corresponds to the separatrices of the pendulum (4.11). Then we have seen that for ϵ small enough the manifolds $W^u(\Pi_\epsilon^0)$ and $W^s(\Pi_\epsilon^{2\pi})$ intersect transversally. On the other hand, one has $E_k < h_1$ and hence the intersection of $W^{u,s}(C_h^\epsilon)$ and $W^{s,u}(R_k(C_{h=1+\epsilon}^\epsilon))$ is also transversal within the energy level $H = h_1$. For $\epsilon = 0.1$, $a_2 = 0.25$ and $d = 0.5$ we represent the invariant manifolds associated with C_h^ϵ in Fig. 6. We clearly observe a transverse intersection between the related manifolds. By means of a Melnikov perturbative techniques [22, 21]

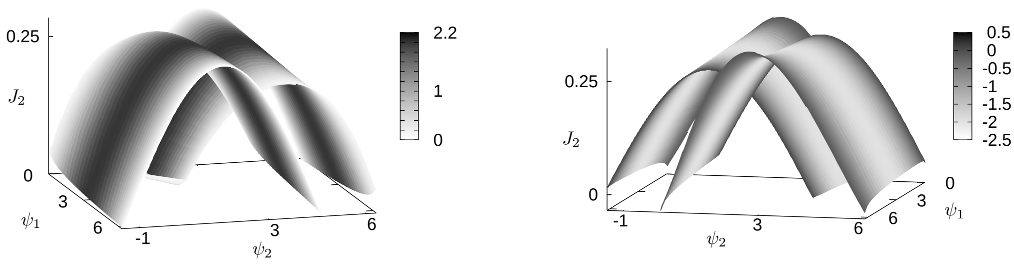

Figure 6: We consider $\epsilon = 0.1$, $a_2 = 0.25$, $d = 0.5$ and $h = 1 + \epsilon$. In the left plot, we show $W^u(C_h^\epsilon)$ and $W^s(R_k(C_{h=1+\epsilon}^\epsilon))$. In the right plot, we show $W^s(C_h^\epsilon)$ and $W^u(R_k(C_{h=1+\epsilon}^\epsilon))$. The grey scale colour in both plots indicates the value of the (omitted in the plots) action J_1.

but dealing with series in the natural parameter $\mu = \sqrt{\epsilon}$, one obtains that the angle between these manifolds is indeed $\mathcal{O}(\mu)$, see [13] for the details.

When we follow the family of periodic orbits C_h^ϵ as the energy h decreases we see the following bifurcation when h decreases crossing E_k: initially $\ell_k \cap W^u(C_h^\epsilon)$ consists of two homoclinic points which collide when $h = E_k$ and disappear. In particular, for $a_2 \notin \mathbb{Z}$, $E_k > h_2$ and there are no primary homoclinic orbits to the hyperbolic elliptic fixed point $p_2 = (0, \pi, 0, 0)$ which is close to the unperturbed pendulum separatrix.

Remark 4.2. *Note, however, that we cannot exclude the existence of multibump homoclinic orbits to p_2 for some values of the parameters. These type of homoclinic trajectories perform several passages close to the NHIM before tend to it asymptotically, see Fig. 13 for a simple example of a 2-bump orbit for a 4D map. We refer to [23, 11, 10] and [24] for different types of multibump homoclinic trajectories.*

4.2 Numerical evidence of non-analyticity of the invariant cylinder

We have seen that model (4.3) and, consequently, the original system described by (4.2) possesses an invariant cylinder Π_ϵ^0 which is normally hyperbolic. At $\epsilon = 0$ this cylinder is analytic. As a rule, it is not an easy task to determine the lack of analyticity and the degree of smoothness of an invariant manifold. This is due to the fact that analyticity is indeed a global property. Our goal in this section is to show how to proceed in order to detect the lack of analyticity of Π_ϵ^0 from a simple numerical experiment. Certainly there are other (more sophisticated) ways to detect non-analyticity. For example, in [25] the non-analyticity of a normally hyperbolic invariant curve was studied in terms of the decay properties of Fourier coefficients. Here, however, our criterion relies simply on a numerical integration of a concrete trajectory. Moreover, an a posteriori check shows that, as it is generically expected, Π^0_ϵ is a $\mathcal{C}^r$-manifold with $r = \tilde\lambda_1/\tilde\lambda_2$ the quotient of the normal and tangent maximal Lyapunov exponents.

First we need to explain the information we are going to use detecting the non-analyticity of the invariant cylinder. We denote by X_H the vector field

$$\begin{array}{ll} \dot\psi_1 = J_1 + a_2 J_2, & \dot\psi_2 = a_2 J_1 + a_3 J_2 \\ \dot J_1 = \sin(\psi_1), & \dot J_2 = \epsilon\sin(\psi_2), \end{array} \tag{4.12}$$

generated by the Hamiltonian (4.2). In the original coordinates of (4.2), the unperturbed invariant cylinder Π^0_0 is given by $\psi_1 = 0, J_1 + a_2 J_2 = 0$. As stated before, Fenichel's normal hyperbolicity theory assures the persistence of a smooth (compact) cylinder Π^0_ϵ for $0 < |\epsilon| < \epsilon_0$ which is generically expected to be non-analytic.

Let us state the basic theoretical facts on which our numerical experiments rely on. The equation (4.12) has an equilibrium at the point $p_1 \in \Pi^0_\epsilon$. Recall that $p_1 = (0,0,0,0)$. The spectrum of the differential of X_H at p_1 is given by $\mathrm{Spec} DX_H(p_1) = \{\tilde\lambda_1, \tilde\lambda_2, -\tilde\lambda_1, -\tilde\lambda_2\}$, where $\tilde\lambda_1 = 1 + a_2^2\epsilon/2 + \mathcal{O}(\epsilon^2)$ and $\tilde\lambda_2 = \sqrt{\epsilon d} + \mathcal{O}(\epsilon^{3/2})$. Denote by $\tilde\Lambda = (\tilde\lambda_1, \tilde\lambda_2)$.

The $2D$ unstable invariant manifold $W^u(p_1)$ of the hyperbolic point p_1 intersects the NHIM Π^0_ϵ transversally and defines an invariant $1D$ submanifold which, from now on, will be denoted by $W^{u,\Pi^0_\epsilon}_{\text{slow}}(p_1)$ to stress that it lies on Π^0_ϵ. This $1D$ submanifold, for $|\epsilon| > 0$, corresponds to the separatrices of the slow pendulum (4.11) within Π^0_ϵ.

We say that an 1D invariant submanifold $W^u_{\text{slow}}(p_1) \subset W^u(p_1)$ is a slow unstable invariant manifold if it is tangent at p_1 to an eigenvector related to the slow eigenvalue $\tilde\lambda_2$. It is easy to see that there are infinitely many slow unstable invariant manifolds. In particular, $W^{u,\Pi^0_\epsilon}_{\text{slow}}(p_1)$ is a slow unstable invariant manifold.

The following two basic observations are essential for our numerical experiments.

1. *If Π^0_ϵ is an analytic manifold then $W^{u,\Pi^0_\epsilon}_{slow}(p_1)$ is analytic.*

   If Π^0_ϵ is an analytic invariant manifold, the restriction of (4.12) onto Π^0_ϵ defines an analytic (Hamiltonian) planar vector field. This planar vector field has a non-degenerated saddle point with eigenvalues $\pm\tilde\lambda_2$

and the corresponding stable and unstable invariant manifolds are one-dimensional and analytic. We note that this unstable manifold must coincide with $W^{u,\Pi^0_\epsilon}_{\text{slow}}(p_1)$ because both lye on Π^0_ϵ and are invariant.

2. *If $\tilde{\Lambda}$ is non-resonant, then there is a unique slow unstable invariant submanifold $W^u_{slow}(p_1)$ which will be denoted by $W^{u,\omega}_{slow}(p_1)$. On the other hand, if $\tilde{\Lambda}$ is resonant then generically all slow unstable submanifolds are non-analytic.*

   The restriction of (4.12) to the $2D$ unstable manifold $W^u(p_1)$ defines a planar analytic vector field with $(0,0)$ as a repulsive fixed point.

   Assume that the eigenvalues $\tilde{\lambda}_1 > \tilde{\lambda}_2 > 0$ of this fixed point are non-resonant, i.e. $\tilde{\lambda}_1/\tilde{\lambda}_2 \in \mathbb{R} \setminus \mathbb{N}$. Then the vector field is analytically conjugated to the linear vector field $\dot{s}_1 = \tilde{\lambda}_1 s_1$, $\dot{s}_2 = \tilde{\lambda}_2 s_2$. The solutions of this linear vector field describe curves which can be parametrized in the form $s_1 = C s_2^{\tilde{\lambda}_1/\tilde{\lambda}_2}$ (or $s_2 = \hat{C} s_1^{\tilde{\lambda}_2/\tilde{\lambda}_1}$), with $C \in \mathbb{R}$ ($\hat{C} \in \mathbb{R}$) a constant, which are non-analytic with the particular exceptions of the solutions $s_1 = 0$ (i.e., $C = 0$) and $s_2 = 0$ (i.e., $\hat{C} = 0$). By the analytic conjugation, the solution with $s_1 = 0$ corresponds to an analytic $W^u_{\text{slow}}(p_1)$. The idea behind our numerics below is to show that this solution is not contained in Π^0_ϵ, meaning that the analytic $W^u_{\text{slow}}(p_1)$ does not coincide with $W^{u,\Pi^0_\epsilon}_{\text{slow}}(p_1)$ and, furthermore, that $W^{u,\Pi^0_\epsilon}_{\text{slow}}(p_1)$ is not analytic.

   If a resonant relation $\tilde{\lambda}_1 = k\tilde{\lambda}_2$, with $k \in \mathbb{N}$, holds, then $\tilde{\Lambda}$ belongs to the so-called Poincaré domain [26]. Such a resonant relation implies, at most, the presence of one resonant term in the normal form of the vector field. Concretely, the restriction of (4.12) to $W^u(p_1)$ can be analytically conjugated (Poincaré's theorem) to

$$\begin{aligned} \dot{s}_1 &= \tilde{\lambda}_1 s_1 + \nu s_2^k, \\ \dot{s}_2 &= \tilde{\lambda}_2 s_2. \end{aligned}$$

   Assuming $\nu \neq 0$, the solutions $s_1 = \nu s_2^k(\log(s_2) + C)/\tilde{\lambda}_2$ describe non-analytic curves, with the only exception of the solution $s_2 = 0$. In particular, any $W^u_{\text{slow}}(p_1)$ is non-analytic, meaning that Π^0_ϵ is also non-analytic. Otherwise, if $\nu = 0$ (degenerate resonant case) all the solutions define analytic curves in the (s_1, s_2)-plane and we expect the manifold Π^0_ϵ to be analytic.

From the previous considerations it follows that:

- If $\tilde{\Lambda}$ is resonant then Π^0_ϵ is generically non-analytic.

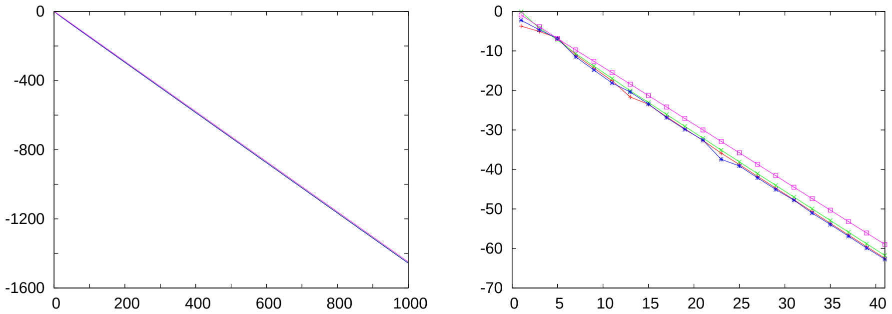

Figure 7: Left: Natural logarithm of the coefficients $\psi_k^{(1)}, \psi_k^{(2)}, J_k^{(1)}, J_k^{(2)}$ for $1 \le k \le 1000$ (k ranges in the x-axis). Right: Detail of the left plot for $1 \le k \le 41$.

- If $\tilde{\Lambda}$ is non-resonant then the analyticity of Π_ϵ^0 implies $W_{\text{slow}}^{u,\Pi_\epsilon^0}(p_1) = W_{\text{slow}}^{u,\omega}(p_1)$ by uniqueness of the analytic invariant unstable manifold.

As a conclusion, we observe that it is enough to consider the generic non-resonant case and to numerically check that the analytic $W_{\text{slow}}^{u,\omega}(p_1)$ leaves the cylinder Π_ϵ^0. Then it follows that $W_{\text{slow}}^{u,\Pi_\epsilon^0}(p_1) \neq W_{\text{slow}}^{u,\omega}(p_1)$ and, consequently, that Π_ϵ^0 is non-analytic. We remark that the tangency order between the analytic solution $s_1 = 0$ and the other solutions of the linear vector field $\dot{s}_1 = \tilde{\lambda}_1 s_1$, $\dot{s}_2 = \tilde{\lambda}_2 s_2$ is $r_* = \tilde{\lambda}_1/\tilde{\lambda}_2$. Hence, in order to detect the difference between the solutions it is necessary to compute an approximation of $W_{\text{slow}}^{u,\omega}(p_1)$ of order $k > r_*$. Numerical errors, due to the use of double precision for example, might imply that a higher order is necessary.

Let us proceed with our numerical experiments. We have considered $a_2 = 0.25$ and $a_3 = 0.5625$ (hence $d = 0.5$). To fix ideas, below we illustrate the lack of analyticity of the NHIM Π_ϵ^0 for $\epsilon = 0.1$. For these values of the parameters one has $\tilde{\lambda}_1 \approx 1.003282954$ and $\tilde{\lambda}_2 \approx 0.222875109$. Then $r_* \approx 4.501547788$ and $\tilde{\Lambda}$ is clearly non-resonant. The slow direction at p_1 is defined by the normalized eigenvector $v_2 \approx (-0.0238567, 0.9068679, -0.1070409, 0.4068951)$. We compute the parametric representation $g(s) = (\psi_1(s), \psi_2(s), J_1(s), J_2(s))$, $s \in \mathbb{R}$, of $W_{\text{slow}}^u(p_1)$. The parameter $s \in \mathbb{R}$ denotes here a local parameter along $W_{\text{slow}}^u(p_1)$ and we look for a series representation of the form $\psi_i(s) = \sum_{k\ge1} \psi_k^{(i)} s^k$, $J_i(s) = \sum_{k\ge1} J_k^{(i)} s^k$, $i = 1, 2$ which (formally) verifies the invariance condition. Uniqueness of the series is obtained by requiring $\|g'(s)\|_2 = 1$, hence the first order coefficients coincide with the components of v_2.

It is a routine task to compute the coefficients $\psi_k^{(i)}, J_k^{(i)}$. The behaviour of the coefficients up to $k = 1000$ is shown in Fig. 7. The symmetries of

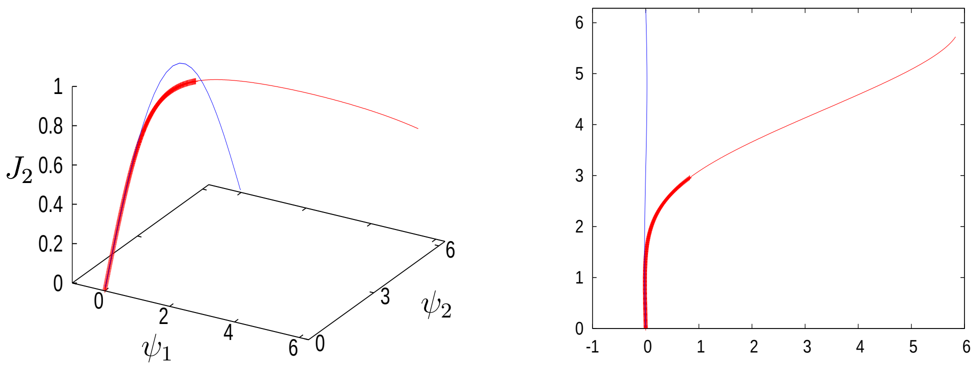

Figure 8: Left: The thick (red) line starting at p_1 corresponds to the analytic $W^u_{\text{slow}}(p_1)$ computed as the sum of the series while the thin (red) line emanating from it correspond to the numerical propagation of the analytic $W^u_{\text{slow}}(p_1)$. The thin line (blue) which stays close to $\psi_1 = 0$ corresponds to $W^{u,\Pi^0_\epsilon}_{\text{slow}}(p_1)$, and hence to a non-analytic $W^u_{\text{slow}}(p_1)$. Right: Projection onto the (ψ_1, ψ_2)-plane of the left figure.

the vector field (4.12) imply that all the coefficients $\psi^{(i)}_k$, $J^{(i)}_k$ vanish for even values of k. Using double precision arithmetic it is enough to consider the coefficients up to $k = 120$. Then one checks that the obtained series give a representation of $W^u_{\text{slow}}(p_1)$ with an error below 10^{-15} for $|s| < s_* \approx 0.3635$. We use values up to $s_* = 0.36$ and we represent for $s < s_*$ the manifold $W^u_{\text{slow}}(p_1)$ by the sum of the series. Finally, we propagate the manifold by integrating the vector field, using a Taylor method, taking as initial condition the sum of the series for $s = s_*$. The trajectory obtained is shown in Fig. 8. The most relevant fact is that the trajectory leaves the neighbourhood of the invariant cylinder, meaning that the computed $W^u_{\text{slow}}(p_1)$ does not coincide with $W^{u,\Pi^0_\epsilon}_{\text{slow}}(p_1)$. This can be checked even from the series representation of the trajectory inside the domain where the representation is accurate, that is, for values of $s < s_*$. In the figure we also represent the homoclinic trajectory lying on Π^0_ϵ. Note that both trajectories are tangent at p_1 as it was expected.

As next step, we look for the parametric representation of the form $g(s_1, s_2) = (\psi_1(s_1, s_2), \psi_2(s_1, s_2), J_1(s_1, s_2), J_2(s_1, s_2))$ of the $2D$ unstable invariant manifold $W^u(p_1)$. That is, we compute the coefficients of the series $\psi_i(s_1, s_2) = \sum_{k,l\geq 1} \psi^{(i)}_{k,l} s_1^k s_2^l$, $J_i(s_1, s_2) = \sum_{k,l\geq 1} J^{(i)}_{k,l} s_1^k s_2^l$, $i = 1, 2$, by (formally) imposing the invariance condition (we normalise the first order coefficients to have $\|(\partial g/\partial s_1)(s_1, s_2)\|_2 = \|(\partial g/\partial s_2)(s_1, s_2)\|_2 = 1$). It turns out

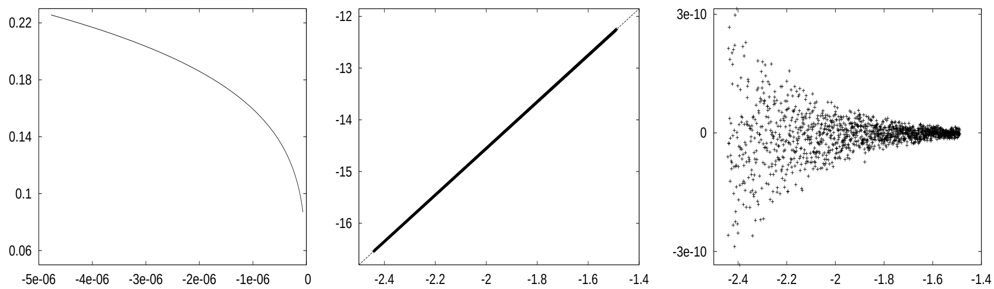

Figure 9: Left: We represent the values of (s_1, s_2) corresponding to the homoclinic trajectory on Π_ϵ^0 (s_1 ranges in the horizontal axis, see text for details). Centre: The points represent $\log(s_1)$, ranging in the vertical axis, as a function of $\log(s_2)$. The thin line represents the function $f(x) = 4.501547787937669\,x - 5.55007880852$. Right: Error $|\log(s_1) - f(\log(s_2))|$ as a function of $\log(s_2)$.

that the truncated series up to order 20 are enough to have a good representation (i.e. with an error below 10^{-15}) of $W^u(p_1)$ for $s = (s_1, s_2)$ in the ball of radius $s_* \approx 0.282$ around p_1, for the values of ϵ, a_2 and d used in this computation.

The direction $s_1 = 0$ corresponds to the analytic slow unstable manifold $W^{u,\omega}_{\text{slow}}(p_1)$. Next, we compute $W^{u,\Pi_\epsilon^0}_{\text{slow}}(p_1)$, that is, we look for the non-analytic $1D$ submanifold of $W^u(p_1)$ within Π_ϵ^0. The homoclinic point which lies on Π_ϵ^0 should have $\psi_1 = 0$, $\psi_2 = \pi$ due to the reversibility of the vector field (4.12). Hence, we take initial conditions $s = (0, s_2)$, with $0 < s_2 < 0.8\, s_*$ and we integrate the corresponding point on $W^u(p_1)$, using a Taylor method with double precision arithmetics, until we reach the Poincaré section $\psi_2 = \pi$, and then we refine s_1 to get $\psi_1 = 0$. The values of s_1, s_2 obtained are shown in Fig. 9, where we also show that $s_1 = s_2^{r_*}$, with $r_* = \tilde\lambda_1/\tilde\lambda_2$. In particular, we clearly see that $W^{u,\Pi_\epsilon^0}_{\text{slow}}(p_1)$ does not coincide with $s_1 = 0$ hence it cannot be analytic.

To sum up, the numerical experiments above provide a strong numerical evidence supporting the following conjecture: for $\epsilon = 0.1$, $a_2 = 0.25$ and $a_3 = 0.5625$, the system (4.12) has a $\mathcal{C}^4$ NHIM Π_ϵ^0 which is not of class $\mathcal{C}^5$.

In a similar way, taking a suitable value of ϵ and under generic conditions, we could provide explicit examples of normally hyperbolic invariant manifolds Π_ϵ^0 of (4.12) which are $\mathcal{C}^r$ but not $\mathcal{C}^{r+1}$.

5 Beyond Normal Form theory: a $4D$ standard-like map

In this section we will describe some numerical results related to a map describing the dynamics at a weak double resonance. Starting from the Hamiltonian function $\mathcal{H}(\psi_1, \psi_2, J_1, J_2)$ in (4.2) we consider the generating function

$$S(\psi_1, \psi_2, J_1, J_2) = \psi_1 \bar{J}_1 + \psi_2 \bar{J}_2 + \delta \mathcal{H}(\psi_1, \psi_2, J_1, J_2).$$

The relations $J_i = \partial S/\partial \psi_i$, $\bar{\psi}_i = \partial S/\partial \bar{J}_i$, $i = 1, 2$, define the family of maps

$$T_\delta : \begin{pmatrix} \psi_1 \\ \psi_2 \\ J_1 \\ J_2 \end{pmatrix} \to \begin{pmatrix} \bar{\psi}_1 \\ \bar{\psi}_2 \\ \bar{J}_1 \\ \bar{J}_2 \end{pmatrix} = \begin{pmatrix} \psi_1 + \delta(\bar{J}_1 + a_2 \bar{J}_2) \\ \psi_2 + \delta(a_2 \bar{J}_1 + a_3 \bar{J}_2) \\ J_1 + \delta \sin(\psi_1) \\ J_2 + \delta\epsilon \sin(\psi_2) \end{pmatrix} \tag{5.1}$$

which can be seen as a $4D$ generalisation of the Chirikov standard map family, see [27].

The map (5.1) has a generic weak double resonance and the dynamics around such a resonance is then approximately described by the Hamiltonian flow X_H in (4.12). Note, however, that the map breaks down the symmetries imposed by the normal form. The following geometrical property is a consequence of this fact. Normal hyperbolicity theory implies that the NHIM Π^0_ϵ, which persists for $0 < |\epsilon| < \epsilon_0$ in the phase space of X_H, also persists into a NHIM $\Pi^0_{\epsilon,\delta}$ within the phase space of the map (5.1) for $0 < |\delta| < \delta_0$. While the separatrices $W^{u,\Pi^0_\epsilon}_{\text{slow}}(p_1)$ and $W^{s,\Pi^0_\epsilon}_{\text{slow}}(p_1)$ for the vector field coincide, it turns out that the separatrices $W^{u,\Pi^0_{\epsilon,\delta}}_{\text{slow}}(p_1)$ and $W^{s,\Pi^0_{\epsilon,\delta}}_{\text{slow}}(p_1)$ of the hyperbolic-hyperbolic point $p_1 = (0, 0, 0, 0)$ corresponding to the slow pendulum within $\Pi^0_{\epsilon,\delta}$ split. We remark that these invariant manifolds (the separatrices) are expected to be non-analytic (see discussion in Section 4.2 concerning the non-analyticity of the related invariant manifolds for the flow).

Note, on the other hand, that this splitting of separatrices has important dynamical consequences because, in particular, it is related to the existence of Arnold diffusion for the map: trajectories can cross through the different Hamiltonian energy surfaces defined by (4.2). Nevertheless, we believe that the role that this splitting plays in the Arnold diffusion is not completely clear nowadays. For example, for $a_2 = 0$ the corresponding manifolds also split but there is not diffusion because the system is uncoupled. In any case, in the following subsection we analyse this splitting of (generically expected non-analytic!) invariant manifolds and we show that asymptotically, for $\delta \to 0$, this splitting has an exponentially small behaviour.

Let us briefly comment on some properties of the map (5.1) that will be used later. The map (5.1) has four fixed points $p_1 = (0,0,0,0)$, $p_2 = (\pi,0,0,0)$, $p_3 = (0,\pi,0,0)$ and $p_4 = (\pi,\pi,0,0)$. We shall consider $\nu = \epsilon d > 0$, $d = a_3 - a_2^2$ (consider $\epsilon \mapsto -\epsilon$ and $\psi_2 \mapsto \psi_2 - \pi$ otherwise). For $\nu > 0$, $|\epsilon| << 1$ and $\delta \lesssim 2$, p_1 is a hyperbolic-hyperbolic point, p_2 is elliptic-hyperbolic, p_3 is hyperbolic-elliptic and p_4 is a totally elliptic fixed point.

Moreover, the map (5.1) is reversible with respect to the planes $\Sigma_{R_1} = \{\psi_1 = 0, \psi_2 = \pi\}$, $\Sigma_{R_2} = \{\psi_1 = \pi, \psi_2 = \pi\}$, and $\Sigma_{R_3} = \{\psi_1 = \pi, \psi_2 = 0\}$. The corresponding reversibilities R_i, $i = 1,\dots,3$ (we recall that F admits the reversibility R if $R \circ F \circ R^{-1} = F^{-1}$) are given by $R_1(\psi_1,\psi_2,J_1,J_2) = (-\psi_1, 2\pi - \psi_2, \bar{J}_1, \bar{J}_2)$, $R_2(\psi_1,\psi_2,J_1,J_2) = (2\pi - \psi_1, 2\pi - \psi_2, \bar{J}_1, \bar{J}_2)$ and $R_3(\psi_1,\psi_2,J_1,J_2) = (2\pi - \psi_1, -\psi_2, \bar{J}_1, \bar{J}_2)$, respectively. The invariant manifolds of the hyperbolic-hyperbolic point $W^{u/s}(p_1)$ generically intersect Σ_{R_i} in a homoclinic point (a fixed point of the reversibility).

In the following sections we are interested in primary homoclinic trajectories to p_1, that is, trajectories which under iteration are asymptotic to p_1 for $n \to \pm\infty$ and without extra passages close to p_1. The points on Σ_{R_i} can have any values of J_1 and J_2 while ψ_1, ψ_2 mod (2π) is one of the following pairs: $(\psi_1,\psi_2) = \{(0,\pi),(\pi,0),(\pi,\pi)\}$. There are two primary homoclinic trajectories with a homoclinic point in Σ_{R_i}, $i = 1,2,3$, one for each pair of branches of the $2D$ manifolds $W^{u/s}(p_1)$. Therefore, there are 6 primary homoclinic trajectories. We show the three basic types of homoclinic trajectories for the values of the parameters $\delta = \epsilon = 0.1$ and $a_2 = 0.25, a_3 = 0.5625$ in the Figs. 10, 11 and 12.

We remark that the trajectory with a homoclinic point in Σ_{R_1} corresponds to the separatrices of the slow pendulum in $\Pi^0_{\epsilon,\delta}$. However, we do not require that the NHIM persists for the values of ϵ considered.

On the other hand, there are infinitely many non-primary homoclinic trajectories with homoclinic points in Σ_{R_2} and Σ_{R_3}. A simple example is shown in Fig. 13.

5.1 Empirical formula for the volume at a homoclinic point on Σ_{R_1}

Let us consider primary homoclinic trajectories having a homoclinic point in Σ_{R_1}, i.e., with $(\psi_1,\psi_2) = (0,\pi)$. See Fig. 10 for an illustration of a homoclinic trajectory like the ones we are considering here.

Denote by $\{\tilde{\lambda}_1, 1/\tilde{\lambda}_1, \tilde{\lambda}_2, 1/\tilde{\lambda}_2\}$, assuming $1 < \tilde{\lambda}_2 < \tilde{\lambda}_1$, the spectrum of the differential matrix of T_δ at p_1. The related eigenvectors $v^{\tilde{\lambda}_1}, v^{\tilde{\lambda}_2}$, generate $W^u(p_1)$. The homoclinic trajectory we look for is tangent to $< v^{\tilde{\lambda}_2} >$. The

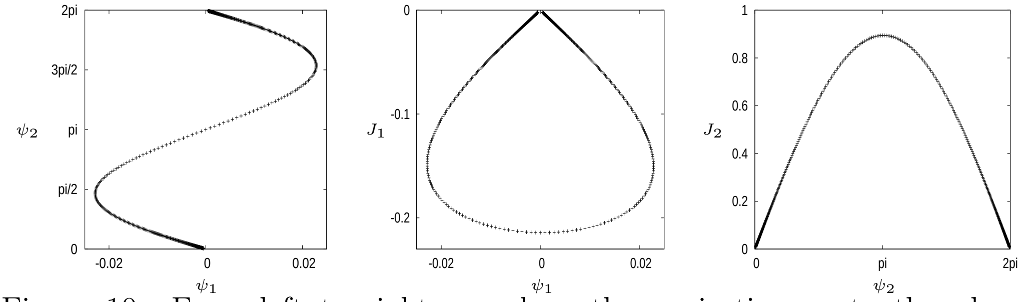

Figure 10: From left to right, we show the projections onto the planes (ψ_1, ψ_2), (ψ_1, J_1) and (ψ_2, J_2) of the primary homoclinic trajectory which has an homoclinic point in Σ_{R_1}.

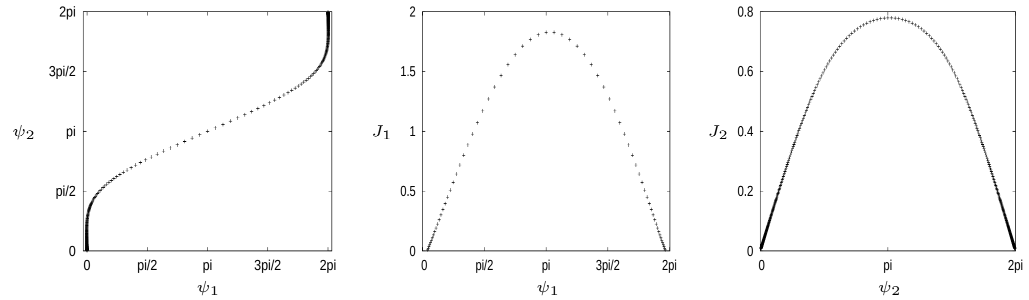

Figure 11: From left to right, we show the projections onto the planes (ψ_1, ψ_2), (ψ_1, J_1) and (ψ_2, J_2) of a primary homoclinic trajectory which has an homoclinic point in Σ_{R_2}, *i.e.* with $(\psi_1, \psi_2) = (\pi, \pi)$.

behaviour of $\tilde{\lambda}_i$, $i = 1, 2$, with respect to δ is given by

$$\begin{aligned} \tilde{\lambda}_1(\delta) &= 1 + \sqrt{(\eta + \sqrt{-4d\epsilon + \eta^2})/2}\; \delta + \mathcal{O}(\delta^2), \\ \tilde{\lambda}_2(\delta) &= 1 + \sqrt{(\eta - \sqrt{-4d\epsilon + \eta^2})/2}\; \delta + \mathcal{O}(\delta^2), \end{aligned} \tag{5.2}$$

where $\eta = 1 + a_3\epsilon$ (recall that $d = a_3 - a_2^2$).

Let $(\psi_1, \psi_2, J_1, J_2) = (G_1(s_1, s_2), G_2(s_1, s_2), G_3(s_1, s_2), G_4(s_1, s_2))$, $s_1, s_2 \in \mathbb{R}$, be the parametrisation of the local unstable $2D$ invariant manifold $W^u(p_1)$. Let p_h be the homoclinic point and consider (s_1^h, s_2^h) such that the point with coordinates $(G_1(s_1^h, s_2^h), G_2(s_1^h, s_2^h), G_3(s_1^h, s_2^h), G_4(s_1^h, s_2^h))$ belongs to the homoclinic trajectory defined by p_h. To measure the splitting of the manifolds at p_h we compute below the volume V defined by the unitary tangent vectors $v_j = \tilde{v}_j / \|\tilde{v}_j\|$ where $\tilde{v}_1(s_1^h, s_2^h) = (\partial G_i/\partial s_1)(s_1^h, s_2^h)$, $\tilde{v}_2(s_1^h, s_2^h) = (\partial G_i/\partial s_2)(s_1^h, s_2^h)$, $\tilde{v}_3(s_1^h, s_2^h) = R_1(\tilde{v}_1(s_1^h, s_2^h))$ and $\tilde{v}_4(s_1^h, s_2^h) = R_1(\tilde{v}_2(s_1^h, s_2^h))$.

The volume V is a well-defined quantity, invariant along the homoclinic trajectory, to compute the distance between the 2D invariant manifolds. We note that, for a fixed ϵ, the angle θ between the vectors v_1 and v_2 is bounded

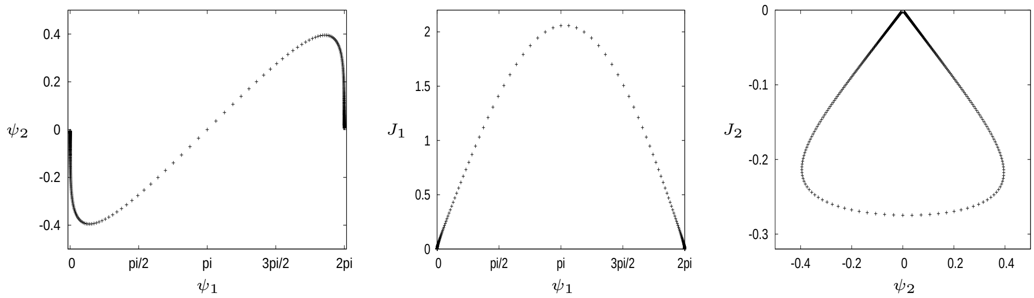

Figure 12: From left to right, we show the projections onto the planes (ψ_1, ψ_2), (ψ_1, J_1) and (ψ_2, J_2) of a primary homoclinic trajectory which has an homoclinic point in Σ_{R_3} with $(\psi_1, \psi_2) = (\pi, 0)$.

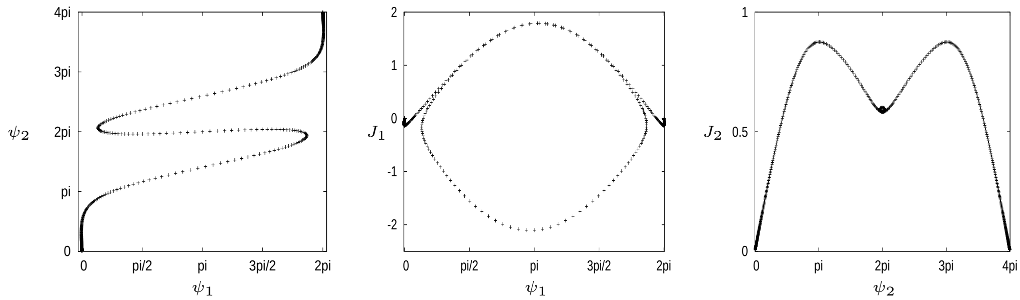

Figure 13: From left to right, we show the projections onto the planes (ψ_1, ψ_2), (ψ_1, J_1) and (ψ_2, J_2) of a non-primary homoclinic trajectory which has an homoclinic point in Σ_{R_3} with $(\psi_1, \psi_2) = (\pi, 2\pi)$. Note that it passes twice close to $\Pi^0_{\epsilon,\delta}$ before it tends asymptotically to p_1.

from below as $\delta \to 0$. Indeed, the map (5.1) tends, as $\delta \to 0$, to the time-1 map associated to the vector field (4.2). Let $R > 0$ be the radius of convergence of the normal form of the vector field on $W^u(p_1)$ around p_1 (see related comments in Section 4.2). Then, taking as initial condition the one corresponding to $s^h = (s_1^h, s_2^h)$ with $\|s^h\| = R/2$, the time t_h to get the homoclinic point p_h is finite. Hence, the time-t_h map defines a diffeomorphism meaning that θ is bounded from below by a quantity depending on ϵ but independent of δ for $\delta \to 0$. For example, for $\epsilon = 0.1$, the behaviour of θ as δ approaches to zero is shown in Fig. 14.

For the numerical computations we use through this section the same parameter values used before

$$a_2 = 0.25 \text{ and } a_3 = 0.5625 \ (d = 0.5), \tag{5.3}$$

and we study the evolution of the volume V with respect to δ for different

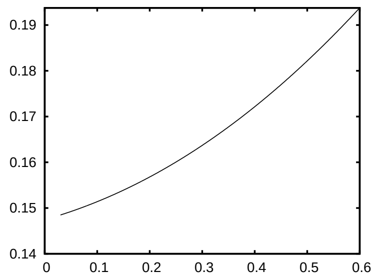

Figure 14: The angle θ (y-axis) as a function of δ (x-axis)for $\epsilon = 0.1$.

values of ϵ. This is shown, for $\epsilon = 0.1, 0.2, \ldots, 0.5$, in Fig. 15.

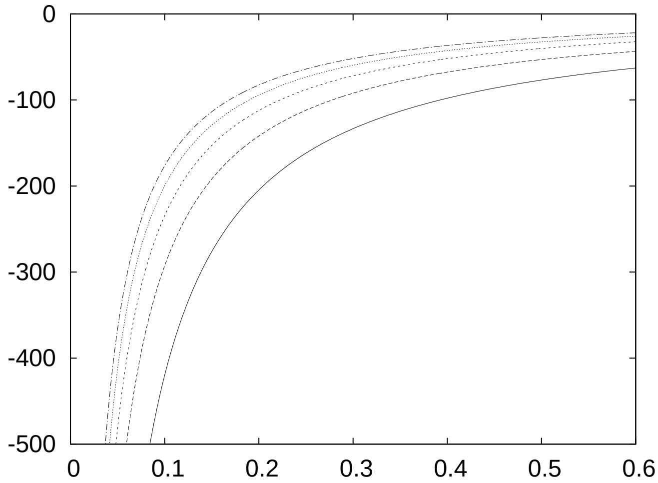

Figure 15: Behaviour of the volume V as a function of δ. In the vertical axis we display the natural logarithm of the volume while δ ranges in the horizontal one. Taking as a reference the line $\log V = -500$, from left to right the lines correspond to $\epsilon = 0.1, 0.2, \ldots, 0.5$ respectively.

Note that, as the map (5.1) is a near-the-identity map, one can construct a non-autonomous vector field periodic with respect to the time, analytic with respect to ψ_1, ψ_2, J_1, J_2, such that the time-one map coincides with the diffeomorphism. This vector field is a slow vector field and, after a suitable scaling and several averaging steps with respect to the time variable, it can be written as an analytic autonomous vector field plus an exponentially small non-autonomous term (see [28, 29]). Moreover, the changes can be made symplectic in order to preserve the symplectic structure (see [30]). In particular, the splitting of the slow stable/unstable separatrices of p_1 should be exponentially small in δ, as it is observed in Fig. 15.

On the other hand, in Section 4.2 we provided a strong evidence of the non-analyticity of the slow manifold Π^0_ϵ of the limit Hamiltonian (4.2), where the slow stable/unstable separatrices of this limit Hamiltonian are contained. A similar reasoning can be applied to the map (5.1), for which a NHIM $\Pi^0_{\epsilon,\delta}$ close to Π^0_ϵ persists for small values of δ. This NHIM is not expected to be analytic neither, hence the restriction $\hat{T}_\delta$ of the family T_δ (5.1) to $\Pi^0_{\epsilon,\delta}$ define a non-analytic family of area-preserving maps. We remark that the classical results on exponentially small upper bounds of the splitting, see [31], require the family of maps to be real-analytic and rely on the width of the analyticity strip of the separatrices of the limit Hamiltonian. Consequently, these results cannot be applied directly to the situation described. Moreover, we do not require the NHIM $\Pi^0_{\epsilon,\delta}$ to exist, in particular we do not know if it persists for the values of ϵ and δ considered below.

Our goal in this section is, however, to give a numerical evidence supporting the fact that the splitting behaves as predicted by the exponentially small upper bounds for the analytic case. In other words, we want to numerically check that the behaviour of the volume V as a function of δ is asymptotically described by an expression of the form

$$V(\delta) \sim A\mu_2^k \mathrm{e}^{-2\pi \mathrm{Im}\hat{\tau}_2/\mu_2} \cos(2\pi \,\mathrm{Re}\,\hat{\tau}_2/\mu_2) \tag{5.4}$$

where $\mu_2 = \log\tilde{\lambda}_2$ (recall that $\tilde{\lambda}_2$ denotes the slow unstable eigenvalue of $DT_\delta(p_1)$ and it is of the form $1 + \mathcal{O}(\delta)$) and $\hat{\tau}_2$ is related to the closest singularity τ_2 to the real axis of the corresponding limit homoclinic trajectory of the limit Hamiltonian (4.2). The symmetries imposed by the Hamiltonian (4.2) imply that the singularity should be on the imaginary axis of complex time, hence $\mathrm{Re}\,\hat{\tau}_2 = 0$ and the volume is not expected to oscillate.

We note that $T_\delta \approx \varphi^H_{t=\delta}$, where φ denotes the flow of the Hamiltonian system defined by (4.2). Consider some fixed values ϵ and δ and assume, for the moment being, that $\Pi^0_{\epsilon,\delta}$ persists for these values. If we denote by $\hat{H}$ the reduction of the Hamiltonian function H to Π^0_ϵ then $\hat{T}_\delta \approx \varphi^{\hat{H}}_{t=\delta}$. The dominant eigenvalue of $\hat{T}_\delta$ is given by $\tilde{\lambda}_2(\delta)$ in (5.2). In order to apply the result in [31] it is necessary to compute the singularity $\hat{\tau}_2$ of the limit flow given by

$$\dot{x} = \frac{1}{\rho}\left(\frac{\partial \hat{H}}{\partial y}\right), \; \dot{y} = \frac{1}{\rho}\left(-\frac{\partial \hat{H}}{\partial x}\right),$$

being $\rho = \sqrt{(\eta - \sqrt{-4d\epsilon + \eta^2})/2}$, $\eta = 1 + a_3\epsilon$, according to (5.2). We remark that, if we consider the vector field generated by the Hamiltonian (4.2) and we denote by τ_2 the singularity of the separatrix solution of the

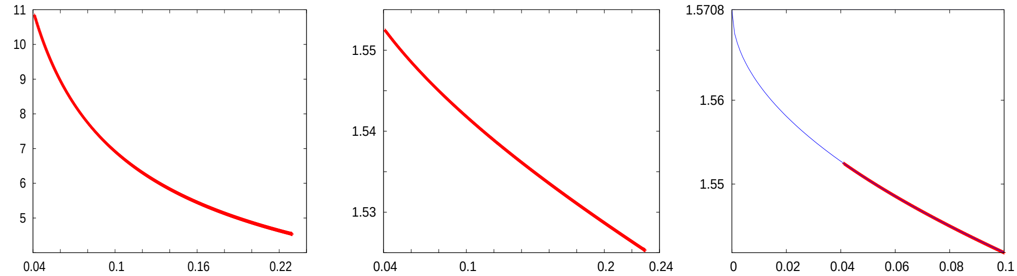

Figure 16: The left plot shows the position of the singularity τ_2 of the limit separatrix related to the slow pendulum of the Hamiltonian (4.2). As before, $a_2 = 0.25$ and $a_3 = 0.5625$. The parameter ϵ ranges on the horizontal axis while $\operatorname{Im}\tau_2$ is displayed in the vertical one. In the centre plot we represent $\hat{\tau}_2 = \rho\tau_2$. In the right plot we observe that $\operatorname{Im}\hat{\tau}_2 \sim \pi/2 + \alpha\sqrt{\epsilon} + \beta\epsilon$ with $\alpha \approx -0.088462$ and $\beta \approx -0.00970047$.

limit homoclinic trajectory which is located closer to the real time axis, then one has $\hat{\tau}_2 = \rho\tau_2$ according to the previous scaling.

The singularity τ_2 can be easily estimate as follows. On the NHIM Π^0_ϵ one has

$$\psi_1 = -\frac{a_2 \sin^2\psi_2}{1 + d^2 J_2^2}\,\epsilon + \mathcal{O}(\epsilon^2), \;\; J_1 = -a_2 J_2 - \frac{d J_2 a_2 \sin\psi_2 \cos\psi_2}{1 + d^2 J_2^2}\,\epsilon + \mathcal{O}(\epsilon^2).$$

The restriction of the Hamiltonian (4.2) to Π^0_ϵ is given by $\hat{H}(\psi_2, J_2) = dJ_2^2/2 + \epsilon\cos(\psi_2) + \mathcal{O}(\epsilon^2)$ (see (4.11)), from which it follows

$$\tau_2 = i\frac{\pi}{2\sqrt{d\epsilon}}\,(1 + \mathcal{O}(\sqrt{\epsilon})). \tag{5.5}$$

We observe that $\rho = \sqrt{d\epsilon}\,(1 + \mathcal{O}(\epsilon))$ and then $\hat{\tau}_2 = i\pi/2 + \mathcal{O}(\sqrt{\epsilon})$.

On the other hand, we have numerically computed the position of the singularity τ_2 of the vector field generated by Hamiltonian (4.2) by a direct integration (using double precision) along the imaginary direction in time. The results are shown in Fig. 16. This way to proceed is independent of the persistence of the NHIM Π^0_ϵ.

To illustrate that the volume V behaves as predicted by (5.4) let us consider $\epsilon = 0.1$. Then, according to (5.2), one has $\tilde{\lambda}_1 \approx 1 + 1.003283\,\delta + \mathcal{O}(\delta^2)$ and $\tilde{\lambda}_2 \approx 1 + 0.222875\,\delta + \mathcal{O}(\delta^2)$. We compute, from the limit homoclinic trajectory of the vector field, the homoclinic point in Σ_{R_1}, which has coordinates $(\psi_1, \psi_2, J_1, J_2) \approx (0, \pi, -0.214258673, 0.89432999)$. Also numerically, one obtains that the singularity is given by $\operatorname{Im}\tau_2 \approx 6.917823$, hence

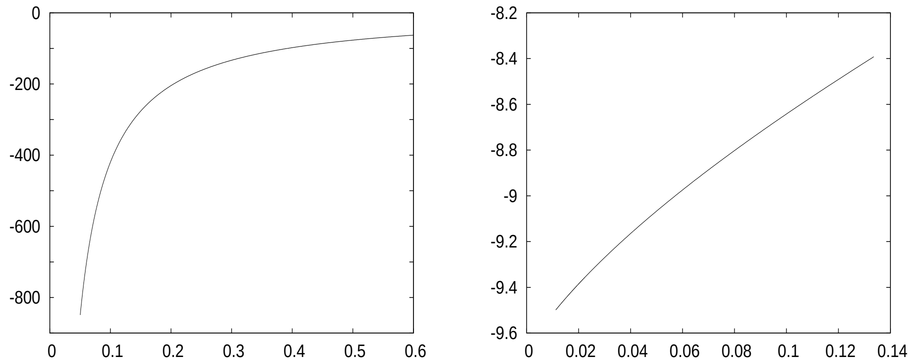

Figure 17: Behaviour of the volume V for $a_2 = 0.25$ and $a_3 = 0.5625$ and $\epsilon = 0.1$. Left plot: we represent $\log V$ as a function of δ (as in Fig. 15). Right plot: we represent $\mu_2 \log V$ (y-axis) as a function of μ_2 (x-axis), $\mu_2 = \log \tilde{\lambda}_2$.

$-2\pi \operatorname{Im} \hat{\tau}_2 \approx -9.6874814$. For $\epsilon = 0.1$ the behaviour of the volume $V(\delta)$ is shown in Fig. 17 left.

Consider $\mu_2 = \log \tilde{\lambda}_2$ and assume that the volume V behaves as $V \sim A\mu_2^B e^{C/\mu_2}$, for suitable real constants A, B and C. From the theoretical considerations one expects $C = -2\pi \operatorname{Im} \hat{\tau}_2 \approx -9.6874814$. Then, $\mu_2 \log V \sim \tilde{A}\mu_2 + B\mu_2 \log \mu_2 + C$, with $\tilde{A} = \log A$. The behaviour of $\mu_2 \log V$ as a function of μ_2 is shown in Fig. 17 right. A fit of $\mu_2 \log V$, for values of $\mu_2 \leq 0.03$, by a function of the form $\tilde{A}\mu_2 + B\mu_2 \log \mu_2 + C$ gives $\tilde{A} \approx 3.51303$, $B \approx -2.96391$ and $C \approx -9.68705$. Moreover, if we fix $B = -3$ and fit the data by a function of the form $\tilde{A}\mu_2 + D\mu_2^2 + B\mu_2 \log \mu_2 + C$ we obtain $\tilde{A} \approx 3.37029$, $D \approx 0.917065$ and $C \approx -9.68739$, even in better agreement with the theoretical value of C.

Next, we keep fixed a_2 and a_3, given by (5.3), but we consider $\epsilon = 0.2$. One has $\operatorname{Im} \tau_2 \approx 4.867549$, $\rho \approx 0.3140576$ and $-2\pi \operatorname{Im} \hat{\tau}_2 \approx -9.60504785$. We look, as before, for an optimal fit $\mu_2 \log V$, for $\mu_2 \leq 0.03$, by a function of the form $\tilde{A}\mu_2 + B\mu_2 \log \mu_2 + C$ and we obtain $\tilde{A} \approx 2.77816$, $B = -3.01843$ and $C = -9.60527$. Again, we observe that $B \approx -3$.

Similar checks have been performed for other ϵ values, all of them supporting the fact that the splitting behaves as predicted by (5.4) and that $B \approx -3$. Some of the results, for values of $\epsilon = 0.1, 0.2, \ldots, 0.5$, are summarised in the table 2.

We conclude that, for $a_2 = 0.25$ and $a_3 = 0.5625$ the behaviour of the volume V agrees with (5.4). Moreover, we conjecture that, for those values of a_2 and a_3, the splitting (in terms of the volume V) of the slow manifolds

ϵ	$\operatorname{Im}\tau_2$	ρ	$-2\pi \operatorname{Im}\hat{\tau}_2$	$\tilde{A}$	B	C
0.1	6.917823	0.2228751	-9.687481	3.51303	-2.96391	-9.68705
0.2	4.867549	0.3140576	-9.605047	2.77816	-3.01843	-9.60527
0.3	3.961189	0.3831117	-9.535223	4.61706	-2.98378	-9.53498
0.4	3.421892	0.4404353	-9.469527	5.95829	-2.99494	-9.46945
0.5	3.054466	0.4900253	-9.404456	6.44125	-2.99815	-9.40443

Table 2: The table contains the numerically computed singularity τ_2, the scaling ρ, the predicted theoretical value $-2\pi \operatorname{Im}\hat{\tau}_2$ and the values $\tilde{A}$, B and C of the fit $\mu_2 \log V \sim \tilde{A}\mu_2 + B\mu_2 \log \mu_2 + C$. See the text for details.

on the NHIM Π^0_ϵ behaves as

$$V \sim \frac{A}{\mu_2^3} \mathrm{e}^{-2\pi \operatorname{Im}\hat{\tau}_2/\mu_2} \tag{5.6}$$

for all the values of ϵ, being $\mu_2 = \log \tilde{\lambda}_2$ and $A \in \mathbb{R}$ a suitable constant. We recall that $\operatorname{Im}\hat{\tau}_2 = \pi/2 + \mathcal{O}(\sqrt{\epsilon})$.

It will be of interest to consider different parameters a_2, a_3 and obtain precise asymptotic formulae of this splitting depending on them. For $a_2 = 0$ the dynamics of the (ψ_2, J_2) variables is uncoupled. After introducing new coordinates $\varphi = \psi_2$, $I = \beta J_2$, with $\beta = \delta a_3$ we get the classical Chirikov standard map $(\varphi, I) \mapsto (\bar{\varphi}, \bar{I}) = (\varphi + \bar{I}, I + k \sin\varphi)$, being $k = a_3\delta^2\epsilon$. The splitting σ for the standard map has been proved to asymptotically behave like $\sigma \sim Ah^{-2}\exp(-\pi^2/h)$, where $h = \mathcal{O}(\sqrt{k})$ (see [32, 33]). For fixed ϵ and a_3 values, one has $h = \mathcal{O}(\delta)$. Going back to the original coordinates (ψ_2, J_2) the splitting behaves like $A\mu_2^B \exp(-C/\mu_2)$ with $B = -3$. We believe that the prefactor A/μ_2^3 in the formula (5.6) holds for all values of a_2 and a_3. Some preliminary numerical checks supporting this fact have been carried out.

5.2 Numerical computation of the volume at a homoclinic point in Σ_{R_2} or in Σ_{R_3}

Let us consider first a primary homoclinic trajectory with a homoclinic point in Σ_{R_2}. The same considerations apply also to an homoclinic trajectory with a homoclinic point in Σ_{R_3} that will be considered later on. See Fig. 11 for an example of a homoclinic trajectory with a homoclinic point in Σ_{R_2}, that is, of the type we are considering here. As far as the authors are aware there is no theoretical framework describing the behaviour of this splitting of the $2D$ manifolds. Hence, in the following we just describe what is observed in the numerical computations concerning the behaviour of the volume V.

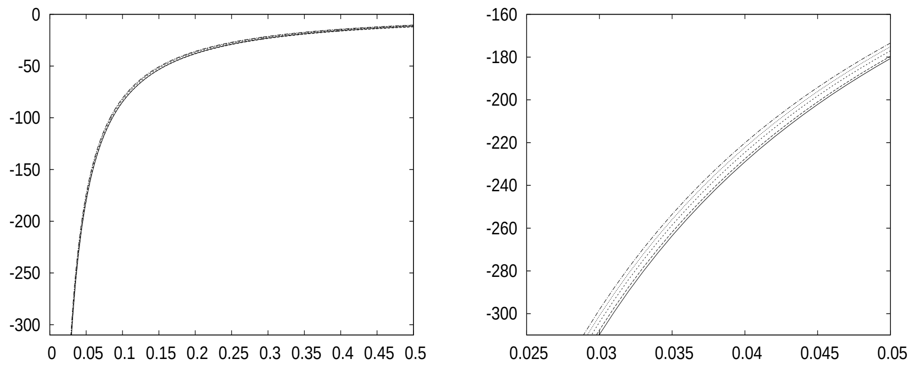

Figure 18: Behaviour of the volume V for $a_2 = 0.25$ and $a_3 = 0.5625$ and $\epsilon = 0.1, 0.2, \ldots, 0.5$ at the homoclinic point with $(\psi_1, \psi_2) = (\pi, \pi)$, see Fig. 11. We represent $\log V$ as a function of δ, we note that the behaviour is very similar for different values of ϵ. The right plot is a magnification of the left one where the five computed volumes can be distinguished. For $\epsilon = 0.1$ we represent $\mu_1 \log V$ (y-axis) as a function of μ_1 (x-axis), where $\mu_1 = \log \tilde{\lambda}_1$.

We remark again that, as the map is near-the-identity, it has a formal integral of motion which, at first order, is given by the Hamiltonian (4.2). Then, the volume $V(\delta)$ computed at an homoclinic point such that $(\psi_1, \psi_2) = (\pi, \pi)$ behaves as an exponentially small function in δ.

The volume V is computed exactly in the same way that was explained in Section 5.1 but, obviously, considering R_2 instead of R_1. The results, for the values (5.3) of a_2, a_3 and for $\epsilon = 0.1$, are shown in Fig. 18. As it is clearly observed, the volume V behaves as exponentially small with respect to δ.

Our next goal is to provide a numerical evidence supporting the fact that $V(\delta)$ behaves indeed as

$$V(\delta) \sim A\mu_1^k \mathrm{e}^{-2\pi \mathrm{Im}\hat{\tau}_1/\mu_1} \tag{5.7}$$

with $\mu_1 = \log(\tilde{\lambda}_1)$ and where $\hat{\tau}_1$ is related (by a factor ρ) to the closest singularity τ_1 of the homoclinic trajectory of the Hamiltonian flow which has a homoclinic point on the plane $(\psi_1, \psi_2) = (\pi, \pi)$.

For $\epsilon = 0.1$, the homoclinic point of the limit trajectory of the Hamiltonian vector field generated by (4.2) is $(\psi_1, \psi_2, J_1, J_2) \approx (\pi, \pi, 1.8290461, 0.7794627)$. Integrating in complex time along the imaginary direction we find the singularity $\tau_1 \approx 1.559370$. According to (5.2), $\rho = \sqrt{(\eta + \sqrt{-4d\epsilon + \eta^2})/2} \approx 1.003282954$, with $\eta = 1 + a_3\epsilon$, hence $\hat{\tau}_1 \approx \rho\tau_1$. In Fig. 19 left we show the behaviour of $\mu_1 \log V$ as a function of μ_1. A fit of $\mu_1 \log(V)$ by a function of the form $\tilde{A}\mu_1 + B\mu_1 \log \mu_1 + C$ in the interval $(0, 0.1)$ gives $\tilde{A} \approx 6.27663$,

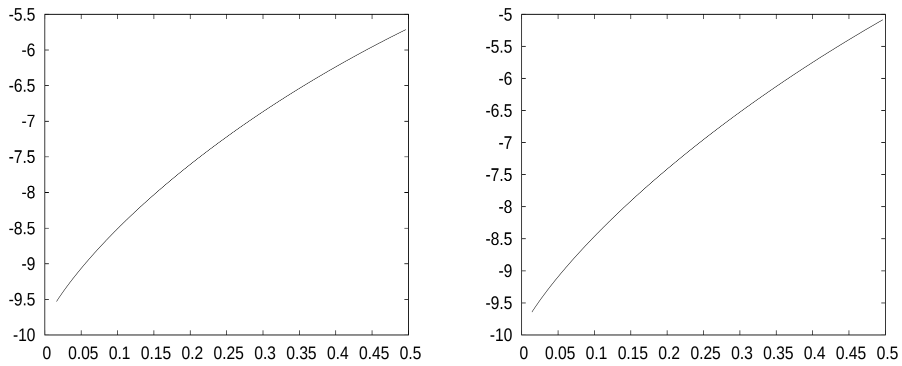

Figure 19: For $\epsilon = 0.1$, $a_2 = 0.25$ and $a_3 = 0.5625$. Behaviour of $\mu_1 \log V$ (y-axis) as a function of μ_1 (x-axis), where $\mu_1 = \log \tilde{\lambda}_1$. The volume V is measured at the homoclinic point on Σ_{R_2} (left) and on Σ_{R_3} (right).

$B \approx -3.01628$ and $C \approx -9.83073$. Again we observe that B is close to -3. Hence, we fix $B = -3$ and perform the fit again to obtain $\tilde{A} \approx 6.30276$ and $C \approx -9.82955$. One checks that the value of C obtained is close to the predicted value $-2\pi \operatorname{Im} \hat{\tau}_1 \approx -9.8299764$.

The table 3 displays the values obtained for values of $\epsilon = 0.1, 0.2, \ldots, 0.5$. We conclude that the exponent $B = -3$ does not depend on ϵ, and we believe that it does not depend on a_2 and a_3 neither.

Having into account that all the computations concerning the position of the singularity have been performed using double precision arithmetics and that the volume V has been computed for values of δ not too close to 0, we think that the fit is precise enough to conclude that the volume $V(\delta)$ behaves as predicted by (5.7) and, more concretely, as

$$V \approx \frac{A}{\mu_1^3} \mathrm{e}^{-2\pi \operatorname{Im} \hat{\tau}_1/\mu_1} \tag{5.8}$$

for a suitable constant $A \in \mathbb{R}$ and where $\mu_1 = \log \tilde{\lambda}_1$.

Concerning the volume $V(\delta)$ computed at a homoclinic point in Σ_{R_3}, we have checked that, for a_2, a_3 from (5.3), it also behaves like (5.8) for a different constant $A \in \mathbb{R}$. For example, for $\epsilon = 0.1$ the homoclinic point of the limit Hamiltonian is located at $(\psi_1, \psi_2, J_1, J_2) \approx (\pi, 0, 2.05923456, -2.74779685)$ and the singularity $\tau \approx 1.57363$. Then, $-2\pi\hat{\tau} \approx -9.91987$. Using the same fit as before for $\delta < 0.08$ one gets $\tilde{A} \approx 7.76753$, $B \approx -3.00716$ and $C \approx -9.93131$. The behaviour of $\mu_1 \log(V)$ as a function of μ_1 is shown in Fig. 19 right. Similar results are obtained for other values of ϵ.

Further investigations are needed to theoretically understand the behaviour of these splittings, the role of the coupling parameter, and the ef-

ϵ	$\mathrm{Im}\,\tau_1$	ρ	$-2\pi\,\mathrm{Im}\,\hat{\tau}_1$	$\tilde{A}$	B	C
0.1	1.559370	1.0032829	-9.829976	6.27663	-3.01628	-9.83073
0.2	1.546355	1.0069100	-9.783173	5.64423	-3.02580	-9.78387
0.3	1.533003	1.0109280	-9.737402	6.59303	-3.01488	-9.73790
0.4	1.519569	1.0153899	-9.694673	6.83096	-3.01273	-9.69492
0.5	1.506144	1.0203554	-9.656013	6.85795	-3.01908	-9.65661

Table 3: The table contains the numerically computed singularity τ_1, the scaling ρ, the predicted theoretical value $-2\pi\,\mathrm{Im}\,\hat{\tau}_1$ and the values $\tilde{A}$, B and C of the fit $\mu_1 \log V \sim \tilde{A}\mu_1 + B\mu_1 \log \mu_1 + C$. See text for details.

fect they have on the diffusion properties. Also the model (5.1) requires much efforts to clarify, for example, the behaviour of the invariant manifolds $W^{u/s}(p_1)$ at the singular limit $\epsilon \to 0$ or at the uncoupled limit $a_2 \to 0$. Moreover, for suitable values of the parameters ϵ, a_2 and a_3 the elliptic-elliptic point p_4 suffers a complex-saddle bifurcation (for a fixed parameters a_2 and a_3 such that $d = a_3 - a_2^2 < 0$ this bifurcation takes place for $\epsilon = (-\gamma \pm \sqrt{\gamma^2 - 4a_3^2}\,)/2a_3^2 < 0$, $\gamma = 2a_3 - 4d$, independently of δ). The dynamical role of the associated invariant manifolds within a double resonance should be investigated. Some of these items will be addressed in future works.

6 Conclusions and outlook

In the paper we have studied double resonances near a totally elliptic fixed point in symplectic 4D maps, providing a clasification and arithmetic properties. In the case of weak resonances of different order it is proved that, generically, the normal form is non-integrable by analysing a truncated model. A NHIM is proved to exist and evidences of the non-analyticity of that manifold, as one can expect, are given. Later on a 4D symplectic family of models, which in the limit tend to behave as the flow normal form is introduced. Several measures of splitting illustrate the main differences with the normal form.

As future work the authors consider relevant to study, first, the case of weak resonances of same order, so that the parameter ϵ in 4.2 and in 5.1 cannot be considered as small. Also the parameter δ in 5.1 can be not very small. The relative positions of the invariant manifolds of the elliptic-hyperbolic points should play then a key role. Other questions worth to consider are the possible bifurcations of the totally elliptic fixed point under changes in ϵ, δ, a_2 and a_3, as well as the role of the definite or non-definite character of the normal form aat the totally elliptic fixed point.

Acknowledgments

This work was partially carried out as a part of an International Joint Project supported by the Royal Society. The final stage of the work was supported in part by the EPSRC grant EP/J003948/1. C.S. and A.V. have been also supported by grants MTM2006-05849/Consolider (Spain), MTM2010-16425 (Spain) and 2009 SGR 67 (Catalonia). The authors are indebted to H.W. Broer and E. Fontich.

References

[1] Nekhoroshev, N. N.; *An exponential estimate of the time of stability of nearly integrable Hamiltonian systems.* Russian Math. Surveys 32 (1977), no. 6, 1–65.

[2] Lochak, P.; Meunier, C.; *Multiphase averaging for classical systems. With applications to adiabatic theorems.* Applied Mathematical Sciences, 72. Springer-Verlag, New York, 1988. xii+360 pp.

[3] Delshams, A.; de la Llave, R.; Seara, Tere M.; *A geometric mechanism for diffusion in Hamiltonian systems overcoming the large gap problem: heuristics and rigorous verification on a model.* Mem. Amer. Math. Soc. 179 (2006), no. 844, viii+141 pp.

[4] Arnold, V.I.; Kozlov, V.V.; Neishtadt, A.I.; *Mathematical aspects of classical and celestial mechanics. Dynamical systems III.* Third edition. Encyclopaedia of Mathematical Sciences, 3. Springer-Verlag, Berlin, 2006.

[5] Laskar, J.; *Frequency analysis for multi-dimensional systems. Global dynamics and diffusion.* Physica D, 67 (1993), 257–281.

[6] P.M. Cincotta, P.M.; Giordano, C.M.; Simó, C.; *Phase space structure of multidimensional systems by means of the Mean Exponential Growth factor of Nearby Orbits (MEGNO).* Physica D, 182 (2003), 151–178.

[7] Froeschlé, C.; Guzzo, M.; Lega, E.; *Local and global diffusion along resonant lines in discrete quasi-integrable dynamical systems* Celestial Mechanics and Dynamical Astronomy, 92 (2005), 243–255.

[8] Froeschlé, C.; Guzzo, M.; Lega, E.; *Measure of the exponential splitting of the homoclinic tangle in four-dimensional symplectic map-*

pings Celestial Mechanics and Dynamical Astronomy, 104 (2009), 191–204.

[9] Arnold, V.I.; *Instability of dynamical systems with many degrees of freedom* Dokl. Akad. Nauk SSSR, 156 (1964), 9–12.

[10] Haller, G.; *Chaos near resonance.* Applied Mathematical Sciences, 138. Springer-Verlag, New York, 1999. 427 pp.

[11] Haller, G.; *Universal homoclinic bifurcations and chaos near double resonances.* J. Statist. Phys. 86 (1997), no. 5-6, 1011–1051.

[12] Todesco, E.; *Local analysis of formal stability and existence of fixed points in* $4d$ *symplectic mappings.* Phys. D 95 (1996), no. 1, 1–12.

[13] Kovacic, G.; *Singular Perturbation Theory for Homoclinic Orbits in a Class of a Near-Integrable Hamiltonian Systems.* Journal of Dynamics and Differential Equations 5 (1993), 559–597.

[14] Haller, G.; Wiggins, S.; *Orbits homoclinic to resonances: the Hamiltonian case.* Phys. D 66 (1993), no. 3-4, 298–346.

[15] Takens, F.; *Forced Oscillations and Bifurcations.* Applications of Global Analysis I. Communications of the Mathematical Institute Rijksuniversiteit Utrecht, 3 (1974).

[16] Broer, H.; *Notes on perturbation theory*, Series of Scientific Monographies "Mathematic and fundamental applications", 1990.

[17] Simó C.; Vieiro A.; *Resonant zones, inner and outer splittings in generic and low order resonances of area preserving maps.* Nonlinearity 22 (2010), no. 5, 1191–1245.

[18] Fenichel, N.; *Persistence and smoothness of invariant manifolds for flows.* Ind. Univ. Math. J. 21 (1971), 193 – 225.

[19] Fenichel, N.; *Asymptotic stability with rate conditions.* Ind. Univ. Math. J. 23 (1974), 1109 – 1137.

[20] Fenichel, N.; *Asymptotic stability with rate conditions II.* Ind. Univ. Math. J. 26 (1977), 81 – 93.

[21] Wiggins, S.; *Global Bifurcations and Chaos.* Applied Mathematical Sciences, 73 (1988), Springer-Verlag, New York.

[22] Guckenheimer, J.; Holmes, P.; *Nonlinear Oscillations, Dynamical Systems and Bifurcations of Vector Fields.* Applied Mathematical Sciences, 42 (1983) Springer-Verlag.

[23] Haller, G.; Wiggins, S.; *N-Pulse Homoclinic Orbits in Perturbations of Resonant Hamiltonian Systems.* Arch. Rational Mech. Anal. 130 (1995), 25 – 101.

[24] Kaper, T.J.; Kovacic, G.; *Multi-bump orbits to resonance bands.* Trans. Amer. Math. Soc. 348(1996), no. 10, 3835 – 3887.

[25] Broer, H.; Simó, C.; Tatjer J.C.; *Towards global models near homoclinic tangencies of dissipative diffeomorphisms.* Nonlinearity, 1998, 11, 667–770.

[26] Arnold, V.I.; *Chapitres supplémentaires de la théorie des équations différentielles ordinaires* Ed. Mir. (1978)

[27] Froeschlé, C.; *The number of isolating integrals in systems with three degrees of freedom* Astrophysics and Space Science, 14 (1971), 110–117.

[28] Neishtadt, A.I.; *The separation of motions in systems with rapidly rotating phase.* J.Appl. Math. Mech., 48 (1984), 133–139.

[29] Broer, H.; Roussarie, R.; Simó, C.; *Invariant circles in the Bogdanov-Takens diffeomorphisms.* Ergod. Th. & Dynam. Sys., 16 (1996), 1147–1172.

[30] Simó, C.; Valls, C.; *A formal approximation of the splitting of separatrices in the classical Arnold's example of diffusion with two equal parameters.* Nonlinearity, 14 (2001), 1707–1760.

[31] Fontich, E; Simó, C.; *The splitting of separatrices for analytic diffeomorphisms.* Ergod. Th. & Dynam. Sys., 10 (1990), 295–318.

[32] Gelfreich, V.G.; *A proof of the exponentially small transversality of the separatrices for the standard map.* Comm. Math. Phys., 201(1) (1999), 155–216.

[33] Lazutkin, V.F.; *Splitting of separatrices for the Chirikov's standard map.* Preprint, http://www.ma.utexas.edu/mp_arc/index-98.html (1998).